t', A STUDY OF THE STABILITY OF
REINFORCED CYLINDRICAL AND CONICAL SHELLS
SUBJECTED TO VARIOUS TYPES AND
COMBINATIONS OF LOADS · SECTION

IV: ,,,

SECTION IV - Matrix Shear Lag
Analysis Utilizing a
High-Speed Digital Computer · Summary
Report, May 1962 — 15 Oct. 1962

by

~~Paul Cooper, Director~~
William K. Rey, ~~Associate~~   Nov. 1962   66 p
refs

University of Alabama Research Institute
George C. Marshall Space Flight Center
(NASA   Contract No. NAS8 - 5012)
transpose date May 28, 1962 - October 15, 1962

(NASA CR-52884) OTS:

MATRIX SHEAR LAG ANALYSIS UTILIZING A HIGH-SPEED DIGITAL COMPUTER

by

William K. Rey

Submitted to

George C. Marshall Space Flight Center

National Aeronautics and Space Administration

This report represents section IV of the summary report for
contract number NAS8-5012

University of Alabama
University, Alabama

November 1962

MATRIX SHEAR LAG ANALYSIS UTILIZING A HIGH-SPEED DIGITAL COMPUTER

by

William K. Rey*

INTRODUCTION

Soon after the introduction of the semi-monocoque type of construction in aircraft, some of the problems encountered in analytically determining the stress distribution in the stressed-skin structure received considerable attention. Accounting for the shear deformations of the skin in determining the distribution of load between the stiffeners and the skin was one of the most difficult problems to solve satisfactorily. This problem of accounting for shear deformations in determining the stress distribution became known as the shear lag problem in the United States and the stress-diffusion problem in Great Britain.

During the late 1930's and early 1940's a number of investigators published fairly rigorous mathematical analyses of the shear lag problem. These mathematical treatments were of limited usefulness for various reasons. In some of these analyses, in order to obtain a solution, an idealized structure or mathematical model was used that did not adequately represent an actual structure. In other analyses, assumptions of infinite length, unusual area variations or a limited number of stiffeners resulted in solutions that were difficult, if not impossible, to apply to a practical structure. The most satisfactory analyses, from the standpoint of adequate representation of the structure, were

*Professor of Aerospace Engineering, University of Alabama.

impractical to use for design purposes due to the large amount of computational effort required.

In 1948, Paul Kuhn of the National Advisory Committee for Aeronautics published a simplified analysis based upon the concept of a substitute single stringer that made possible the analysis of multistringer panels with a minimum of computational effort. Since 1948, the simplified analysis proposed by Kuhn has been widely accepted and used throughout the aircraft industry. However, since the Kuhn analysis requires the use of empirical relations that were obtained from a very limited experimental program, some questions have arisen concerning the use of the Kuhn analysis for certain types of structures.

By using high-speed digital computers, it is now possible to perform detailed structural analyses that were formerly impractical due to the large computational effort required. In general, in order to utilize a digital computer for this purpose, it is necessary to use matrix methods adapted to the specific structure.

In this report, a brief discussion of some of the early efforts to solve the shear lag problem is presented. After discussing some of the early work, an analysis of the shear lag problem based upon the Maxwell-Mohr Method is presented. Using matrix methods, this Maxwell-Mohr analysis is adapted for solution by a high-speed digital computer. In one of the appendices, two numerical examples are presented in which the Maxwell-Mohr analysis is applied to the thrust structure of the C-5 launch vehicle. Recommendations for further study and investigation of the shear lag problem are given.

REVIEW OF PREVIOUS WORK

A survey of the readily available literature was conducted as a means of becoming familiar with the work of other investigators who have studied the shear lag problem. The results of this survey are presented as references 1 through 54. Although this list of references is not a complete list of all published articles relating to shear lag, it is believed to include the major contributions that have been published in the English language.

One of the first, if not the first, published discussions of the shear lag problem was presented in Great Britain by Winny in reference 54. Winny considered the distribution of the normal stress in the unstiffened skin of a wing between two spars subjected to a known spanwise bending moment distribution. Winny obtained a Fourier series solution for the differential equations of equilibrium. In Great Britain, the work of Winny was followed by that of Argyris in references 3 through 6, Cox in references 11 through 13, Duncan in reference 16, Fine in references 19 and 20, Goodey in reference 22, Smith in reference 50 and Williams in references 52 and 53. Three of the most comprehensive discussions are those of Argyris in reference 57, Cox in reference 13 and Goodey in reference 22.

In Germany, Ebner considered the shear lag problem at about the same time as early investigators in Great Britain and the United States. Two of Ebner's papers were translated and are available as references 17 and 18.

In the United States, some of the first published solutions of the shear lag problem were those of Kuhn in references 29 through 32,

4

Lovett in reference 39, Reissner in reference 43 and Sibert in reference 49. Kuhn followed his early work with a number of other publications and in reference 36 presented one of the most comprehensive discussions of shear lag effects that is currently available. Other important contributions are those of Borsari in reference 8, Chiarito in references 9 and 10, Duberg in reference 15, Hildebrand in references 24 and 25, Hoff in references 26 and 27, Kempner in reference 28, Levy in reference 37, Reissner in references 45 and 46 and White in reference 51.

Unfortunately, the large majority of the solutions presented in the references cited above are not directly applicable to a multi-stiffened structure with tapered flanges such as the thrust structure of the C-5 launch vehicle. A number of investigators have obtained exact solutions for a panel consisting of only one stiffener plus a flange to which the load is applied. When the same type of analysis is applied to a panel containing more than one stiffener, the labor involved in performing the analysis and obtaining a solution increases very rapidly. Furthermore, the expressions obtained for the stress distributions become considerably more complex and awkward to use. To illustrate the rapid increase in complexity with the number of stiffeners, an exact analysis of a panel consisting of two stiffeners in addition to the flange is presented in Appendix A. This analysis is the same as that presented by Kuhn in reference 36 for a single stiffener. Note that this analysis may also be applied to a stiffened cylinder if the proper areas are used in computing the shear lag parameters.

The one analysis that is ralatively simple to apply to a multi-string-

er stiffened panel is the analysis of Kuhn based upon the concept of a substitute single stringer as presented in references 35 and 36. Since the application of the substitute single stringer analysis requires the use of empirical relations that were determined from the results of a limited experimental program, further study of this method is desirable.

In addition to the analytical and experimental studies mentioned above, the electrical analogy solutions presented by Newton in reference 41 and Ross in reference 47 are of particular interest. These electrical analogies make it practical to apply some of the more rigorous analytical solutions to a practical structure.

A brief survey of the literature relating to the application of matrix methods in structural analysis was also conducted. The results of this literature search are presented as references 55 through 98.

MATRIX ANALYSIS OF STIFFENED PANEL

A shear lag analysis based upon the application of the Maxwell-Mohr Method appears to offer a number of advantages over some of the other analyses. Since an analysis based upon the Maxwell-Mohr Method is readily adapted to matrix notation, solutions may be obtained utilizing a digital computer. Therefore, after a computer program has been written for the analysis, it should be possible to obtain future solutions with a minimum expenditure of time and effort. This procedure would make possible the consideration of a number of alternate designs for the purpose of obtaining a minimum weight design. Wehle and Lansing in reference 98 and Bruhn in reference 61 have shown how this type of analysis may be applied to a variety of structures.

The application of the Maxwell-Mohr Method requires that the actual structure be replaced by an idealized structure composed of simple structural elements. For a multi-stringer stiffened panel, there are at least two immediately apparent choices for the idealized structure. In one case, the idealized structure may be visualized as being composed of sheet elements that transmit only shearing forces plus stiffeners that transmit only normal forces. The area of each stiffener in this idealized structure may be taken as the actual stiffener area plus the area of an equivalent width of sheet that acts with the stiffener in resisting the normal forces. An idealized structure of this type is used in the numerical example of Method I presented in Appendix E. An alternate choice for the idealized structure may be made by distributing the stiffener areas over the sheet to produce an equivalent unstiffened panel. Since there are no stiffeners in

this idealized structure, the equivalent sheet material must resist both shearing and normal forces. A numerical example using this type of structure is presented as Method II in Appendix E. The notation employed throughout Appendix E is the same as that used by Bruhn in reference 61.

In adapting the Maxwell-Mohr Method for solution by matrix algebra, it is necessary to have analytical expressions for the flexibility coefficients. These flexibility coefficients are denoted by the symbol a_{ij} and correspond to the displacement at the point i due to a unit change in force at the point j. Wehle and Lansing in reference 98 have obtained analytical expressions for the flexibility coefficients of a variety of structural elements. These expressions for the flexibility coefficients are also given by Bruhn in reference 61.

In reference 98, Wehle and Lansing present the flexibility coefficients for a bar with a tapering area subjected to a uniformly varying axial force. These flexibility coefficients are expressed in terms of parameters that are functions of the taper ratio. However, Wehle and Lansing do not give the analytical expressions for these parameters although they do represent them in graphical form. In order to utilize a computer to generate the elements in a matrix of flexibility coefficients, it is necessary to have functional expressions for these parameters instead of graphical representations. Therefore, analytical expressions for the flexibility coefficients of a tapered bar are derived in Appendices B and C. In Appendix B, a bar having a linearly tapering area is considered. In Appendix C.

a bar having linearly varing dimensions is considered.

The equivalent sheet analysis presented as Method II in Appendix E requires the use of flexibility coefficients for a panel subjected to a uniformly varying shear flow. Since this type of loading was not considered in any of the references consulted, expressions for the flexibility coefficients of a panel subjected to a uniformly varying shear flow are derived in Appendix D.

In the analyses presented as Methods I and II in Appendix E, the sheet material was assumed to be capable of transmitting the loads without buckling. It may be possible to use the analysis of Method I in the presence of buckling by an appropriate reduction in the width of sheet assumed to act with each stiffener in resisting compressive forces. However, this would introduce additional uncertanties. The analysis presented as Method II in Appendix E would be difficult to apply in the presence of buckling.

The analysis presented as Method II in Appendix E has the advantage of providing a more detailed stress distribution immediately adjacent to the flange or post where the stress gradient is largest. Both analyses have the disadvantage of requiring the inversion of high-order matrices.

CONCLUDING REMARKS

The results obtained in the numerical examples of Appendix E illustrate the use of the Maxwell-Mohr Method in performing a shear lag analysis of a complex structure. These results also demonstrate the need of a high-speed digital computer to fully utilize the analytical procedures presently available. However, these results do not represent the ultimate solution to the shear lag problem. Further study of the application of the Maxwell-Mohr Method is necessary in which different choices of the idealized structure are made. The application of this method to a panel containing cut-outs or discontinuities should be investigated. Furthermore, some of the rigorous analyses such as those employing stress functions should be investigated to determine the feasibility of adapting other analyses to digital computer solutions.

The available published literature contains very little useful experimental data. Additional experimental data are required to compare the stress distributions obtained analytically with actual stress distributions.
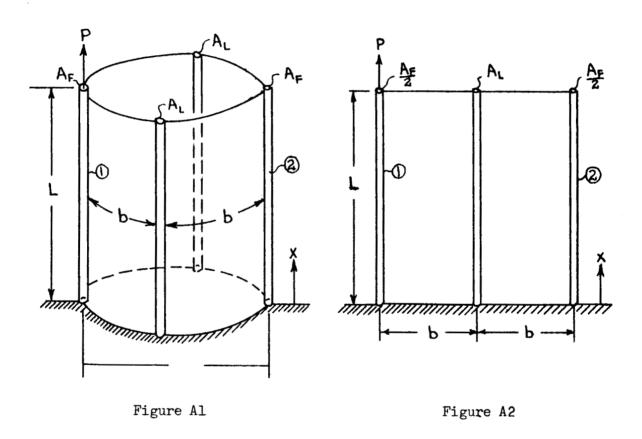
The possibility of utilizing one of the available solutions in a minimum-weight analysis should be investigated. However, this study should probably be delayed until an adequate experimental program has determined the most satisfactory analytical solution.

A number of these areas requiring further study will be investigated in the performance of contract NAS8-5168.

APPENDIX A

STRESS DISTRIBUTION FOR UNSYMMETRICAL LOADING

For the cylinder shown in figure A1 or the flat panel shown in figure A2, expressions may be derived for the normal stresses in the flanges and stiffeners and the shearing stresses in webs assuming an infinite transverse stiffness. These are the type of expressions referred to by Kuhn on page 123 of reference 36.

Figure A1   Figure A2

In both figures the load D is applied to flange 1 and the web thickness is t.
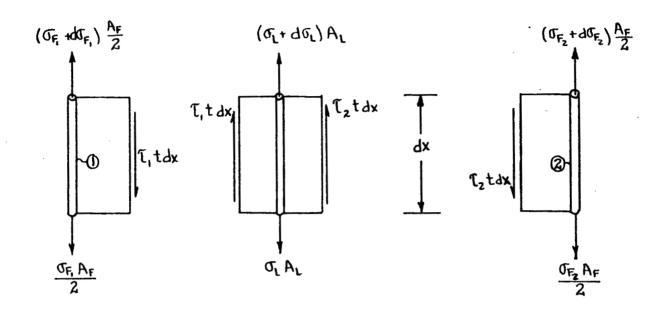
Figure A3

From the free-body diagrams of figure A3, the following equations of equilibrium are obtained:

$$\frac{d\sigma_{F_1}}{dx} = \frac{2t}{A_F} \tau_1 \qquad \text{(Eq.A1)}$$

$$\frac{d\sigma_L}{dx} = -\frac{t}{A_L} (\tau_1 + \tau_2) \qquad \text{(Eq.A2)}$$

$$\frac{d\sigma_{F_2}}{dx} = \frac{2t}{A_F} \tau_2 \qquad \text{(Eq.A3)}$$

where, σ_{F_1} is the normal stress in flange 1

σ_{F_2} is the normal stress in flange 2

τ_1 is the shearing stress in the web between flange 1 and the stiffener (A_L)

τ_2 is the shearing stress in the web between flange 2 and the stiffener (A_L).

The relationships between the shearing stresses, τ_1 and τ_2, and the normal stresses, σ_{F_1}, σ_{F_2} and σ_L are

12

$$\frac{d\tau_1}{dx} = \frac{G}{Eb} (\sigma_{F_1} - \sigma_L) \qquad (Eq.A4)$$

$$\frac{d\tau_2}{dx} = \frac{G}{Eb} (\sigma_{F_2} - \sigma_L) \qquad (Eq.A5)$$

Differentiating equations A4 and A5 with respect to x and substituting equations A1, A2 and A3 in the result yields

$$\frac{d^2\tau_1}{dx^2} = \frac{Gt}{Eb} \left(\frac{\tau_1}{A_F} + \frac{\tau_1 + \tau_2}{A_L} \right) \qquad (Eq.A6)$$

and

$$\frac{d^2\tau_2}{dx^2} = \frac{Gt}{Eb} \left(\frac{\tau_2}{A_F} + \frac{\tau_1 + \tau_2}{A_L} \right) \qquad (Eq.A7)$$

Defining $A_T = A_F + A_L$, equations A6 and A7 become

$$\frac{d^2\tau_1}{dx^2} = \frac{Gt}{Eb} \left(\frac{A_T}{A_F A_L} \tau_1 + \frac{1}{A_L} \tau_2 \right) \qquad (Eq.A8)$$

$$\frac{d^2\tau_2}{dx^2} = \frac{Gt}{Eb} \left(\frac{1}{A_L} \tau_1 + \frac{A_T}{A_F A_L} \tau_2 \right) \qquad (Eq.A9)$$

Shear lag parameters K_1 and K_2 are defined as

$$K_1 = \sqrt{\frac{Gt}{Eb} \left(\frac{A_T}{A_F A_L} \right)} = \sqrt{\frac{Gt}{Eb} \left(\frac{1}{A_F} + \frac{1}{A_L} \right)} \qquad (Eq.10)$$

$$K_2 = \sqrt{\frac{Gt}{Eb} \left(\frac{1}{A_L} \right)} \qquad (Eq.11)$$

Equations A8 and A9 may now be written as

$$\frac{d^2\tau_1}{dx^2} - K_1^2 \tau_1 - K_2^2 \tau_2 = 0 \qquad (Eq.12)$$

$$\frac{d^2\tau_2}{dx^2} - K_2^2 \tau_1 - K_1^2 \tau_2 = 0 \qquad (Eq.13)$$

Solving equation A12 for τ_2 and substituting in equation A13

$$\frac{d^4\tau_1}{dx^4} - 2K_1^2 \frac{d^2\tau_1}{dx^2} + (K_1^4 - K_2^4)\, \tau_1 = 0 \qquad \text{(Eq.A14)}$$

Equation A14 has a solution of the form

$$\tau_1 = C_1 \exp m_1 x + C_2 \exp m_2 x + C_3 \exp m_3 x + C_4 \exp m_4 x^* \qquad \text{(Eq.A15)}$$

where C_1, C_2, C_3, and C_4 are constants to be determined from the boundary conditions and m_1, m_2, m_3, and m_4 are the roots of the equation

$$m^4 - 2K_1^2 m^2 + K_1^4 - K_2^4 = 0.$$

The roots are

$$m_{1,2} = \pm\sqrt{K_1^2 + K_2^2} = \pm K_3$$

$$m_{3,4} = \pm\sqrt{K_1^2 - K_2^2} = \pm K_4$$

Substituting these roots, equation A15 becomes

$$\tau_1 = C_1 \exp K_3 x + C_2 \exp(-K_3 x) + C_3 \exp K_4 x + C_4 \exp(-K_4 x)$$

$$\text{(Eq.A16)}$$

Substituting equation A16 into equation A12 and solving for τ_2,

$$\tau_2 = C_1 \exp K_3 x - C_2 \exp(-K_3 x) - C_3 \exp K_4 x + C_4 \exp(-K_4 x)$$

$$\text{(Eq.A17)}$$

The boundary conditions are:

(1) At $x = 0$, $\tau_1 = 0$

(2) At $x = 0$, $\tau_2 = 0$

(3) At $x = L$, $\sigma_{F_1} = \dfrac{P}{A_F}$ and $\sigma_L = 0$

(4) At $x = L$, $\sigma_{F_2} = 0$ and $\sigma_L = 0$

Applying the boundary conditions to equations A16 and A17 yields, after simplification,

---

* The notation exp u denotes e^u.

$$C_1 = -C_4 = \frac{G}{2Eb}\left(\frac{P}{A_F}\right)\left(\frac{1}{K_3 \exp K_3 L + K_4 \exp(-K_4 L)}\right)$$

(Eq.A18)

$$C_2 = -C_3 = -\frac{G}{2Eb}\left(\frac{P}{A_F}\right)\left(\frac{1}{K_3 \exp(-K_3 L) + K_4 \exp K_4 L}\right)$$

(Eq.A19)

Substituting equations A18 and A19 into equations A16 and A17 yields

$$\tau_1 = \frac{G}{2Eb}\left(\frac{P}{A_F}\right)\frac{\exp K_3 x - \exp(-K_4 x)}{K_3 \exp K_3 L + K_4 \exp(-K_4 L)} - \frac{G}{2Eb}\left(\frac{P}{A_F}\right)\frac{\exp(-K_3 x) - \exp K_4 x}{K_3 \exp(-K_3 L) + K_4 \exp K_4 L}$$

(Eq.A20)

$$\tau_2 = \frac{G}{2Eb}\left(\frac{P}{A_F}\right)\frac{\exp K_3 x - \exp(-K_4 x)}{K_3 \exp K_3 L + K_4 \exp(-K_4 L)} + \frac{G}{2Eb}\left(\frac{P}{A_F}\right)\frac{\exp(-K_3 x) - \exp K_4 x}{K_3 \exp(-K_3 L) + K_4 \exp K_4 L}$$

(Eq.A21)

The shearing stresses τ_1 and τ_2 given by equations A20 and A21 may also be expressed in terms of hyperbolic functions as:

$$\tau_1 = \frac{G}{Eb}\left(\frac{P}{A_F}\right)\frac{K_3\left[\sinh(K_3 L - K_3 x) - \sinh(K_3 L + K_4 x)\right] + K_4\left[\sinh(K_3 x + K_4 L) - \sinh(K_4 L - K_4 x)\right]}{K_3^2 + K_4^2 + 2K_3 K_4 \cosh(K_3 L + K_4 L)}$$

(Eq.A22)

$$\tau_2 = \frac{G}{Eb}\left(\frac{P}{A_F}\right)\frac{K_3\left[\cosh(K_3 L - K_3 x) - \cosh(K_3 L + K_4 x)\right] + K_4\left[\cosh(K_3 x + K_4 L) - \cosh(K_4 L - K_4 x)\right]}{K_3^2 + K_4^2 + 2K_3 K_4 \cosh(K_3 L + K_4 L)}$$

(Eq.A23)

Substituting equations A20 and A21 into equations A1, A2 and A3, yields, after integration,

$$\sigma_{F_1} = \frac{GPt}{EbA_F^2}\left[\frac{\frac{1}{K_3}\exp K_3 x + \frac{1}{K_4}\exp(-K_4 x)}{K_3 \exp K_3 L + K_4 \exp(-K_4 L)} + \frac{\frac{1}{K_3}\exp(-K_3 x) + \frac{1}{K_4}\exp K_4 x}{K_3 \exp(-K_3 L) + K_4 \exp K_4 L}\right] + C_5$$

(Eq.A24)

$$\sigma_{F_2} = \frac{GPt}{EbA_F^2}\left[\frac{\frac{1}{K_3}\exp K_3 x + \frac{1}{K_4}\exp(-K_4 x)}{K_3 \exp K_3 L + K_4 \exp(-K_4 L)} - \frac{\frac{1}{K_3}\exp(-K_3 x) + \frac{1}{K_4}\exp K_4 x}{K_3 \exp(-K_3 L) + K_4 \exp K_4 L}\right] + C_6 \qquad \text{(Eq.A25)}$$

$$\sigma_L = -\frac{GPt}{EbA_F A_L}\left[\frac{\frac{1}{K_3}\exp K_3 x + \frac{1}{K_4}\exp(-K_4 x)}{K_3 \exp K_3 L + K_4 \exp(-K_4 L)}\right] + C_7 \qquad \text{(Eq.A26)}$$

After applying the boundary conditions to evaluate C_5, C_6 and C_7, these equations become

$$\sigma_{F_1} = \frac{P}{A_F}\left\{1 + \frac{2Gt}{EbA_F}\left[\frac{\cosh(K_3 L - K_3 x) + \cosh(K_4 L - K_4 x) + \frac{K_4}{K_3}\cosh(K_3 x + K_4 L) + \frac{K_3}{K_4}\cosh(K_3 L + K_4 x) - \left(\frac{K_3}{K_4} + \frac{K_4}{K_3}\right)\cosh(K_3 L + K_4 L) - 2}{K_3^2 + K_4^2 + 2K_3 K_4 \cosh(K_3 L + K_4 L)}\right]\right\} \qquad \text{(Eq.A27)}$$

$$\sigma_{F_2} = \frac{2GPt}{EbA_F^2}\frac{-\sinh(K_3 L - K_3 x) + \sinh(K_4 L - K_4 x) + \frac{K_3}{K_4}\left[\sinh(K_3 L + K_4 L) - \sinh(K_3 L + K_4 x)\right] - \frac{K_4}{K_3}\left[\sinh(K_3 L + K_4 L) - \sinh(K_3 x + K_4 L)\right]}{K_3^2 + K_4^2 + 2K_3 K_4 \cosh(K_3 L + K_4 L)} \qquad \text{(Eq.A28)}$$

16

$$\sigma_L = \frac{PGt}{EbA_F A_L} \left[\frac{\frac{1}{K_3} (\exp K_3 L - \exp K_3 x) + \frac{1}{K_4} \exp (-K_4 L) - \exp (-K_4 x)}{K_3 \exp K_3 L + K_4 \exp (-K_4 L)} \right]$$

(Eq.A29)

Equations A22 and A23 for the shearing stresses combined with equations A27, A28, and A29 for the normal stresses completely describe the stress distribution in the cylinder of figure A1 or the flat panel of figure A2.

APPENDIX B

FLEXIBILITY COEFFICIENTS FOR A BAR WITH A LINEARLY TAPERING AREA
SUBJECTED TO A UNIFORMLY VARYING AXIAL FORCE

In order to fully utilize computer capabilities to generate the
elements in a matrix of flexibility coefficients, it is necessary to
obtain algebraic expressions for the flexibility coefficients. Wehle
and Lansing in reference 98 have developed expressions for the flexi-
bility coefficients of members subjected to various loadings. How-
ever, they do not give algebraic expressions for the flexibility
coefficients of a bar with a linearly tapered area subjected to a
uniformly varying axial force. In this appendix, the necessary alge-
braic expressions are derived. The notation employed is the same as
that used by Bruhn and Schmitt in reference 61.

Consider the bar shown in figure B1 in which the area varies
linearly from A_i to A_j.
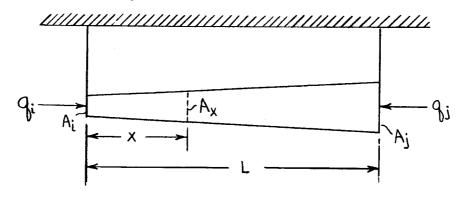
Figure B1

The area A_x at a distance x from the area A_i may be expressed as

$$A_x = A_i + \frac{x}{L}(A_j - A_i).$$
(Eq. B1)

If the shear flow in the web attached to the bar is assumed constant, the force in the bar, q_x, at station x may be expressed as

$$q_x = q_i + \frac{x}{L}(q_j - q_i). \qquad \text{(Eq.B2)}$$

The strain energy in the bar is given by

$$U = \frac{1}{2E}\int_0^L \frac{q_x^2}{A_x}\,dx. \qquad \text{(Eq.B3)}$$

and the flexibility coefficients are given by

$$\left.\begin{aligned}
a_{ij} &= a_{ji} = \frac{\partial^2 U}{\partial q_i \partial q_j}\\[2ex]
a_{ii} &= \frac{\partial^2 U}{\partial q_i^2}\\[2ex]
a_{jj} &= \frac{\partial^2 U}{\partial q_j^2}
\end{aligned}\right\} \qquad \text{(Eqs.B4)}$$

Substituting the expressions for q and given by equations B2 and B3 into equations B4, the equations for the flexibility coefficients become

$$\left.\begin{aligned}
a_{ij} &= a_{ji} = \frac{1}{EL}\int_0^L \frac{x\,dx}{A_x} - \frac{1}{EL^2}\int_0^L \frac{x^2 dx}{A_x}\\[2ex]
a_{ii} &= \frac{1}{E}\int_0^L \frac{dx}{A_x} - \frac{2}{EL}\int_0^L \frac{x\,dx}{A_x} + \frac{1}{EL^2}\int_0^L \frac{x^2 dx}{A_x}\\[2ex]
a_{jj} &= \frac{1}{EL^2}\int_0^L \frac{x^2 dx}{A_x}
\end{aligned}\right\} \qquad \text{(Eqs.B5)}$$

Denoting the area ratio $\dfrac{A_i}{A_j}$ by c, equations B5 become, after integration

$$a_{ij} = a_{ji} = \frac{L}{6A_iE} \; \phi_{ij}$$

$$a_{ii} = \frac{L}{3A_iE} \; \phi_{ii}$$

$$a_{jj} = \frac{L}{3A_iE} \; \phi_{jj}$$

(Eqs. B6)

where,

$$\phi_{ij} = \frac{6c}{(1-c)^2} \left(\frac{c+1}{2} + \frac{c}{1-c} \ln c \right)$$

$$\phi_{ii} = \frac{-3c}{(1-c)^3} \left(\frac{c^2-4c+3}{2} + \ln c \right)$$

$$\phi_{jj} = \frac{3c}{(1-c)^3} \left(\frac{3c^2-4c+1}{2} - c^2\ln c \right)$$

(Eqs. B7)

In Table B1, values of the parameters ϕ_{ii}, ϕ_{jj} and ϕ_{ij} are tabulated for 0.01 increments of c from 0.10 to 0.90. In figure B2, the ϕ parameters are plotted versus the area ratio c.

Table B1

Flexibility Coefficient Parameters for a Linearly Tapering Area

c	ϕ_{ii}	ϕ_{jj}	ϕ_{ij}	c	ϕ_{ii}	ϕ_{jj}	ϕ_{ij}
0.05	0.2790	0.0719	0.1221	0.51	0.8231	0.5889	0.6904
0.10	0.4105	0.1391	0.2179	0.52	0.8284	0.5984	0.6985
0.11	0.4312	0.1521	0.2351	0.53	0.8335	0.6078	0.7064
0.12	0.4506	0.1649	0.2518	0.54	0.8386	0.6171	0.7143
0.13	0.4689	0.1776	0.2681	0.55	0.8435	0.6264	0.7221
0.14	0.4862	0.1901	0.2839	0.56	0.8483	0.6356	0.7299
0.15	0.5026	0.2026	0.2992	0.57	0.8529	0.6448	0.7376
0.16	0.5181	0.2149	0.3142	0.58	0.8579	0.6540	0.7449
0.17	0.5329	0.2271	0.3288	0.59	0.8626	0.6631	0.7523
0.18	0.5471	0.2391	0.3431	0.60	0.8670	0.6721	0.7596
0.19	0.5606	0.2511	0.3570	0.61	0.8714	0.6811	0.7669
0.20	0.5736	0.2629	0.3706	0.62	0.8758	0.6900	0.7741
0.21	0.5860	0.2747	0.3839	0.63	0.8800	0.6989	0.7812
0.22	0.5979	0.2863	0.3969	0.64	0.8842	0.7078	0.7882
0.23	0.6094	0.2979	0.4097	0.65	0.8884	0.7166	0.7951
0.24	0.6205	0.3093	0.4222	0.66	0.8924	0.7253	0.8020
0.25	0.6312	0.3207	0.4344	0.67	0.8964	0.7340	0.8088
0.26	0.6415	0.3320	0.4464	0.68	0.9002	0.7426	0.8158
0.27	0.6515	0.3431	0.4582	0.69	0.9037	0.7511	0.8229
0.28	0.6611	0.3542	0.4698	0.70	0.9068	0.7593	0.8305
0.29	0.6705	0.3652	0.4811	0.71	0.9118	0.7685	0.8352
0.30	0.6795	0.3762	0.4923	0.72	0.9155	0.7770	0.8417
0.31	0.6883	0.3870	0.5033	0.73	0.9191	0.7854	0.8481
0.32	0.6968	0.3978	0.5140	0.74	0.9227	0.7939	0.8544
0.33	0.7051	0.4084	0.5246	0.75	0.9262	0.8022	0.8607
0.34	0.7132	0.4190	0.5351	0.76	0.9297	0.8106	0.8669
0.35	0.7210	0.4296	0.5453	0.77	0.9331	0.8189	0.8730
0.36	0.7286	0.4400	0.5554	0.78	0.9365	0.8272	0.8791
0.37	0.7360	0.4504	0.5653	0.79	0.9398	0.8354	0.8851
0.38	0.7432	0.4607	0.5752	0.80	0.9431	0.8436	0.8911
0.39	0.7503	0.4710	0.5848	0.81	0.9463	0.8517	0.8970
0.40	0.7572	0.4811	0.5943	0.82	0.9494	0.8598	0.9029
0.41	0.7639	0.4913	0.6036	0.83	0.9524	0.8677	0.9087
0.42	0.7704	0.5013	0.6128	0.84	0.9555	0.8753	0.9145
0.43	0.7768	0.5113	0.6219	0.85	0.9586	0.8834	0.9202
0.44	0.7831	0.5212	0.6309	0.86	0.9616	0.8915	0.9258
0.45	0.7892	0.5311	0.6398	0.87	0.9646	0.8996	0.9314
0.46	0.7951	0.5408	0.6485	0.88	0.9676	0.9077	0.9370
0.47	0.8010	0.5506	0.6571	0.89	0.9705	0.9156	0.9425
0.48	0.8067	0.5603	0.6656	0.90	0.9734	0.9234	0.9480
0.49	0.8123	0.5699	0.6740	0.95	0.9872	0.9619	0.9750
0.50	0.8178	0.5794	0.6822	1.00	1.0000	1.0000	1.0000

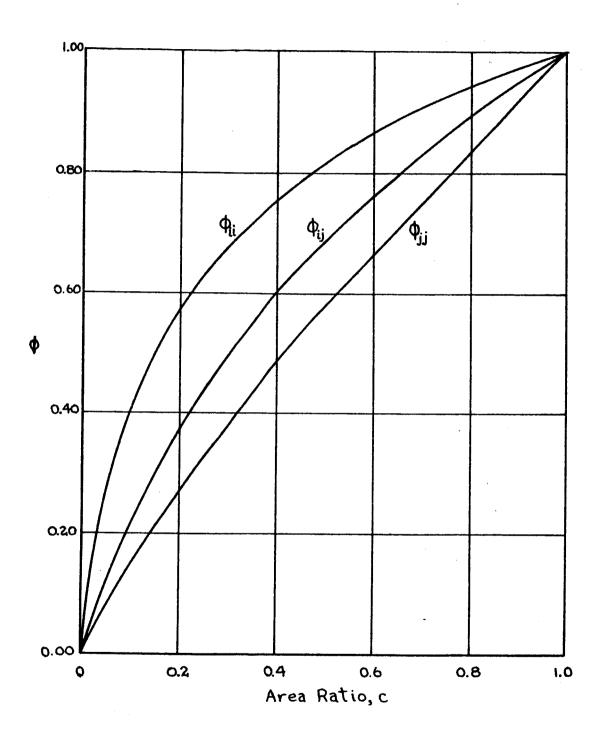Flexibility Coefficient Parameters for A Linearly Tapering Area

Figure B2

APPENDIX C

FLEXIBILITY COEFFICIENTS FOR A BAR WITH LINEARLY VARYING DIMENSIONS SUBJECTED TO A UNIFORMLY VARYING AXIAL FORCE

In this appendix, algebraic expressions are derived for the flexibility coefficients for a bar in which the typical cross-sectional dimension, such as the diameter of a round rod or width of a square bar, varies linearly over the length of the bar. The bar shown in figure C1 is assumed to be subjected to a constant shear flow so that the axial force in the bar varies uniformly throughout the length. As in Appendix B, the notation employed is the same as that used by Bruhn and Schmitt in reference 61.
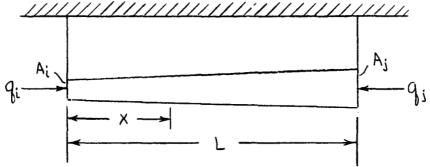

Figure C1

The equations for the normal force in the bar at any station and for the total strain energy stored in the bar are given in Appendix B by equations B2 and B3. If b_i is the value of the typical dimension at $x = 0$ and b_j the balue at $x = L$, the value b_x at station x is given by

$$b_x = b_i + \frac{x}{L}(b_j - b_i) \qquad (Eq.C1)$$

The expressions for the flexibility coefficients in terms of the area will be the same as those given in Appendix B by equations B5. The integration is performed noting that the area may be expressed as

$$A_x = Kb_x^2 = K\left[b_i + \frac{x}{L}(b_j - b_i)\right]^2 \qquad (Eq.C2)$$

where K depends upon the cross-sectional shape. Again denoting the area ratio $\frac{A_i}{A_j}$ by C, the expressions for the flexibility coefficients are

$$\left.\begin{array}{l} a_{ij} = \dfrac{L}{6A_iE}\ \phi_{ij} \\[2ex] a_{ii} = \dfrac{L}{3A_iE}\ \phi_{ii} \\[2ex] a_{jj} = \dfrac{L}{3A_iE}\ \phi_{jj} \end{array}\right\} \qquad (Eqs.C3)$$

where

$$\phi_{ij} = 6\left\{\frac{c}{(1-c)^2}\left[\sqrt{c}-1+\ln\left(\frac{1}{\sqrt{c}}\right)\right] + \frac{c^{3/2}}{(1-\sqrt{c})^3}\left[\sqrt{c}-\frac{1}{\sqrt{c}}+\ln\frac{1}{c}\right]\right\}$$

$$\phi_{ii} = 3\left\{\sqrt{c}+\frac{2c}{(1-\sqrt{c})^2}\left[1-\sqrt{c}-\ln\left(\frac{1}{\sqrt{c}}\right)\right] - \frac{c^{3/2}}{(1-\sqrt{c})^3}\left[\sqrt{c}-\frac{1}{\sqrt{c}}+\ln\frac{1}{c}\right]\right\}$$

$$\phi_{jj} = 3\left[\frac{c^{3/2}}{(1-\sqrt{c})^3}\left(\frac{1}{\sqrt{c}}-\sqrt{c}-\ln\frac{1}{c}\right)\right] \qquad (Eqs.C4)$$

In Table C1, values of the parameters ϕ_{ii}, ϕ_{jj} and ϕ_{ij} are tabulated for 0.01 increments of c from 0.10 to 0.90. In figure C2, the ϕ parameters are plotted versus the area ratio c.

Table C1

Flexibility Coefficient Parameters for Linearly Varying Dimensions

c	ϕ_{ii}	ϕ_{jj}	ϕ_{ij}	c	ϕ_{ii}	ϕ_{jj}	ϕ_{ij}
0.05	0.4015	0.0898	0.1795	0.51	0.8379	0.5984	0.7061
0.10	0.5100	0.1613	0.2774	0.52	0.8424	0.6075	0.7135
0.11	0.5264	0.1746	0.2940	0.53	0.8468	0.6165	0.7207
0.12	0.5416	0.1876	0.3100	0.54	0.8512	0.6255	0.7279
0.13	0.5560	0.2005	0.3252	0.55	0.8555	0.6345	0.7349
0.14	0.5694	0.2131	0.3400	0.56	0.8600	0.6436	0.7414
0.15	0.5822	0.2255	0.3542	0.57	0.8650	0.6531	0.7468
0.16	0.5943	0.2377	0.3680	0.58	0.8678	0.6609	0.7560
0.17	0.6057	0.2498	0.3814	0.59	0.8719	0.6697	0.7628
0.18	0.6167	0.2617	0.3944	0.60	0.8758	0.6784	0.7696
0.19	0.6272	0.2734	0.4070	0.61	0.8797	0.6871	0.7763
0.20	0.6373	0.2850	0.4193	0.62	0.8836	0.6957	0.7829
0.21	0.6469	0.2965	0.4313	0.63	0.8874	0.7043	0.7895
0.22	0.6563	0.3078	0.4431	0.64	0.8911	0.7129	0.7960
0.23	0.6652	0.3190	0.4545	0.65	0.8948	0.7214	0.8025
0.24	0.6739	0.3301	0.4657	0.66	0.8985	0.7299	0.8088
0.25	0.6822	0.3411	0.4766	0.67	0.9023	0.7384	0.8151
0.26	0.6903	0.3520	0.4874	0.68	0.9057	0.7468	0.8214
0.27	0.6982	0.3628	0.4979	0.69	0.9091	0.7552	0.8277
0.28	0.7058	0.3735	0.5082	0.70	0.9125	0.7635	0.8339
0.29	0.7132	0.3840	0.5183	0.71	0.9159	0.7718	0.8401
0.30	0.7204	0.3946	0.5283	0.72	0.9193	0.7801	0.8462
0.31	0.7274	0.4051	0.5378	0.73	0.9226	0.7993	0.8523
0.32	0.7341	0.4153	0.5477	0.74	0.9259	0.7965	0.8583
0.33	0.7407	0.4255	0.5571	0.75	0.9291	0.8046	0.8643
0.34	0.7472	0.4357	0.5664	0.76	0.9324	0.8128	0.8701
0.35	0.7535	0.4458	0.5756	0.77	0.9356	0.8210	0.8759
0.36	0.7596	0.4558	0.5846	0.78	0.9386	0.8280	0.8819
0.37	0.7657	0.4657	0.5934	0.79	0.9418	0.8371	0.8876
0.38	0.7717	0.4757	0.6019	0.80	0.9449	0.8452	0.8932
0.39	0.7773	0.4854	0.6108	0.81	0.9479	0.8531	0.8989
0.40	0.7829	0.4951	0.6193	0.82	0.9509	0.8611	0.9045
0.41	0.7884	0.5048	0.6277	0.83	0.9539	0.8691	0.9100
0.42	0.7938	0.5144	0.6360	0.84	0.9569	0.8771	0.9155
0.43	0.7991	0.5240	0.6442	0.85	0.9599	0.8850	0.9209
0.44	0.8042	0.5335	0.6523	0.86	0.9629	0.8929	0.9263
0.45	0.8094	0.5430	0.6601	0.87	0.9658	0.9008	0.9316
0.46	0.8146	0.5525	0.6676	0.88	0.9687	0.9087	0.9368
0.47	0.8192	0.5616	0.6759	0.89	0.9716	0.9166	0.9420
0.48	0.8240	0.5709	0.6836	0.90	0.9745	0.9244	0.9472
0.49	0.8287	0.5801	0.6912	0.95	0.9880	0.9629	0.9750
0.50	0.8334	0.5893	0.6987	1.00	1.0000	1.0000	1.0000

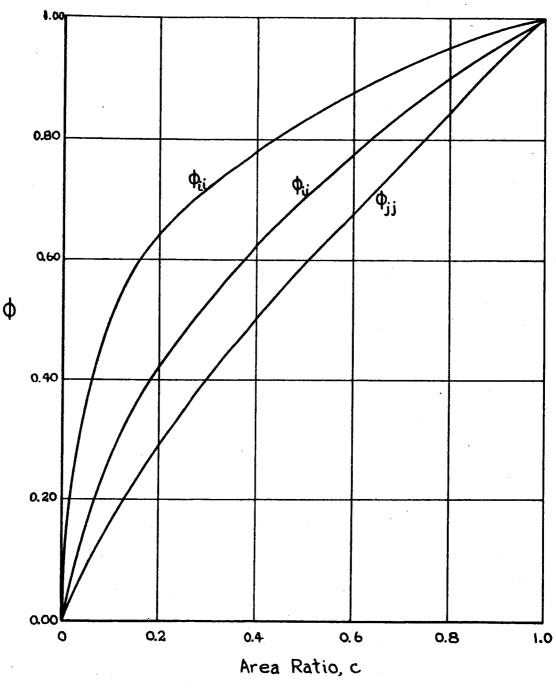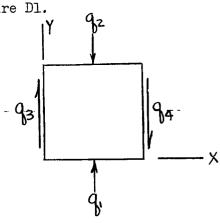Flexibility Coefficient Parameters for Linearly Varying Dimensions

Figure C2

APPENDIX D

FLEXIBILITY COEFFICIENTS FOR A PANEL SUBJECTED TO A UNIFORMLY
VARYING SHEAR FLOW

In this appendix, algebraic expressions are derived for the flexibility coefficients for a panel element simultaneously subjected to a uniformly varying shear flow and a uniformly varying axial force as shown in figure D1.

Figure D1

Panel thickness = t

Bruhn and Schmitt in reference 61 give the flexibility coefficients for the axial forces as

$$a_{11} = a_{22} = \frac{L}{3AE} = \frac{h}{3btE}$$

$$a_{12} = a_{21} = \frac{L}{6AE} = \frac{h}{6btE} \quad .$$

Assuming a linear variation in the shear flow,

$$q_x = q_3 + \frac{x}{b}(q_4 - q_3)$$

where q_x is the shear flow at station x. The strain energy of shear may be expresses as

$$dU_{shear} = \frac{1}{2}\frac{\tau^2}{G} \, dx \, dy$$

where τ is the shearing stress.

Since the shear flow is assumed constant in the y-direction, the strain energy becomes

$$U_{shear} = \frac{ht}{2G} \int_0^b \tau^2 \, dx$$

$$= \frac{h}{2Gt} \left\{ q_3^2 \int_0^b \left(1 - \frac{2x}{b} + \frac{x^2}{b^2} \right) dx + q_4^2 \int_0^b \frac{x^2}{b^2} \, dx + 2q_3 q_4 \int_0^b \left(\frac{x}{b} - \frac{x^2}{b^2} \right) dx \right.$$

After integrating and substituting S = bh, the expressions for the flexibility coefficients are

$$a_{33} = a_{44} = \frac{S}{3Gt}$$

$$a_{34} = a_{43} = \frac{S}{6Gt}$$

APPENDIX E

NUMERICAL EXAMPLES

In this appendix, two numerical examples are presented in which the Maxwell-Mohr Method employing matrix notation is used to determine the stress distribution in the thrust structure of the C-5 launch vehicle for the rebound loading condition. A typical section, representing the stiffened panel from one of the hold-down posts to an adjacent thrust post, is shown in figure E1. The typical section is assumed to be a flat panel having a width equal to the arc length of the curved panel. The material for both the sheet and the stiffeners is 7075-T6 aluminum alloy having a Modulus of Elasticity, E, of 10,500,000 psi and a Modulus of Rigidity, G, of 4,000,000 psi.

Method I
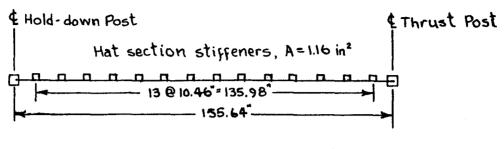
The analysis used in the first numerical example is referred to as Method I. In this analysis, the idealized structure is assumed to consist of a hold-down post to which the load is applied that transmits only normal stresses, stiffeners that transmit only normal stresses and sheet material that transmits only shearing stresses. The generalized force system used in the Method I analysis is shown in figure E2. In figure E2, q_1 through q_8 represent the normal force in the hold-down post at the indicated stations, q_9 through q_{106} represent the normal force in the stiffeners at the indicated locations and q_{107} through q_{204} represent the shear flow in the indicated web. In figure E3, the generalized force system is shown in greater detail

for the element in bay 3 between the fifth and sixth stiffeners.

The hold-down post is assumed to have a linearly varying area in each bay. Within each bay, the shear flow in the sheet is assumed to be constant between adjacent stiffeners. As a result of the latter assumption, the normal forces in the hold-down post and in the stiffeners vary linearly between stations.

The idealized structure assumes that the total strain energy consists of the sum of the following: (1) the strain energy due to the normal forces in the hold-down post, (2) the strain energy in the skin due to the normal forces acting parallel to the stiffeners, (3) the strain energy due to the shear flow in the skin, and, (4) the strain energy due to the normal forces in the stiffeners. The strain energy due to the normal forces in the skin is accounted for by assuming that the stiffeners in the idealized panel have an area equal to the area of the actual stiffeners plus the area of the equivalent width of sheet. In this idealized panel, the strain energies due to the following forces are neglected: (1) normal forces in the skin acting perpendicular to the stiffeners, (2) forces in the thrust post, (3) shearing forces in the posts and stiffeners, and, (4) forces in the intermediate rings. This analysis also assumes that the upper ring assembly effectively serves as a rigid support.

Typical Section of Stiffened Panel

¢ Hold-down Post ¢ Thrust Post
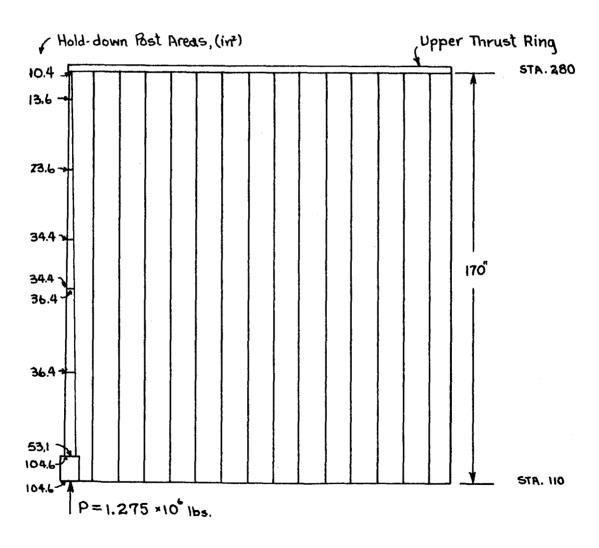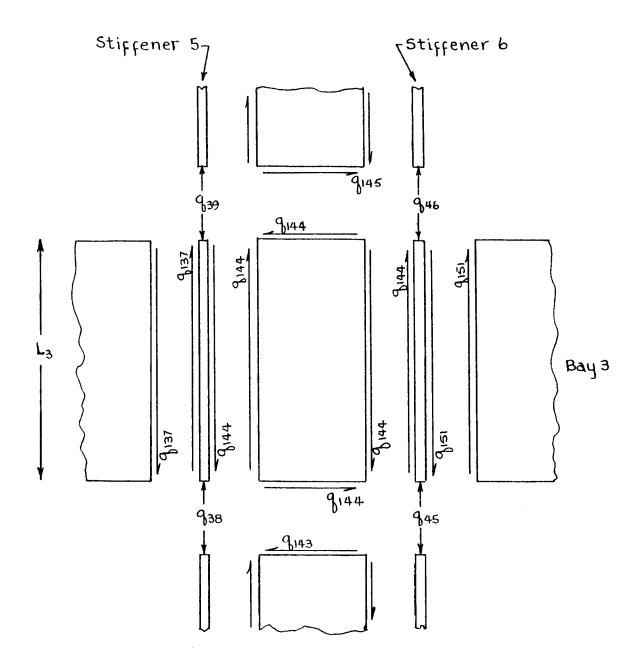
Hat section stiffeners, $A = 1.16$ in^2

|← 13 @ 10.46" = 135.98" →|

|← 155.64" →|

Sheet Thickness = 0.32"

Hold-down Post Areas, (in^2) Upper Thrust Ring

10.4 STA. 280

13.6

23.6

34.4

34.4
36.4

36.4

170"

53.1
104.6

104.6 STA. 110

P = 1.275 × 10^6 lbs.

Figure E1

Generalized Force System for Method I

Figure E2

Details of Generalized Force System for Method I

For stiffener 5: $q_{39} = q_{38} + (q_{137} - q_{144})L_3$

For stiffener 6: $q_{46} = q_{45} + (q_{144} - q_{151})L_3$

Figure E3

Details of Hold-down Post
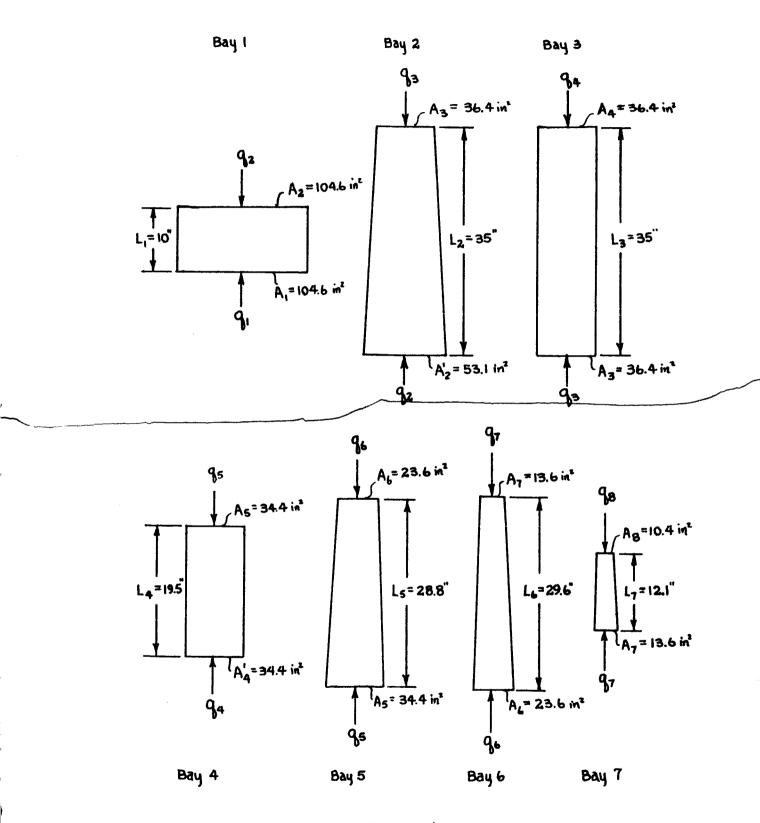

Figure E4

Using the notation employed in reference 61, the matrix of flexibility coefficients is a symmetrical matrix denoted by $\begin{bmatrix} a_{ij} \end{bmatrix}$. For the panel shown in figure E2,

$$
\begin{bmatrix} a_{ij} \end{bmatrix} = \begin{bmatrix}
a_{1,1} & a_{1,2} & a_{1,3} \cdots \cdots a_{1,204} \\
a_{2,1} & a_{2,2} & a_{2,3} \cdots \cdots a_{2,204} \\
\cdot & & \cdot \\
\cdot & & \cdot \\
\cdot & & \cdot \\
\cdot & & \cdot \\
\cdot & & \cdot \\
\cdot & & \cdot \\
a_{204,1} & a_{204,2} & a_{204,3} \cdots \cdots a_{204,204}
\end{bmatrix}
\qquad \text{(Eq.E1)}
$$

As indicated, since the generalized force system contains 204 generalized forces, the $\begin{bmatrix} a_{ij} \end{bmatrix}$ matrix is a 204 x 204 matrix.

The elements in the matrix of flexibility coefficients that correspond to the generalized forces q_1 through q_8 acting in the hold-down post are computed using equations B6 and B7 derived in Appendix B. The notation used in computing the flexibility coefficients for the hold-down post is illustrated in figure E4. Referring to figure E4 for the necessary dimensions, these flexibility coefficients are:

$$
a_{1,1} = \frac{L_1}{3A_1 E} \qquad \text{(Eq.E2)}
$$

$$
a_{1,2} = a_{2,1} = \frac{L_1}{6A_1 E} \qquad \text{(Eq.E3)}
$$

$$
a_{2,2} = \frac{L_1}{3A_1 E} + \frac{L_2}{3A_3 E} \, 0_{22} \qquad \text{(Eq.E4)}
$$

where $\quad \phi_{22} = \dfrac{3c_{23}}{(1-c_{23})^3} \left(\dfrac{3c_{23}^2 - 4c_{23} + 1}{2} - c_{23}^2 \ln c_{23} \right)$

and $\quad c_{23} = \dfrac{A_3}{A_2}$

$$a_{2,3} = a_{3,2} = \dfrac{L_2}{6A_3 E} \phi_{23} \qquad\qquad \text{(Eq.E5)}$$

where $\quad \phi_{23} = \dfrac{6c_{23}}{(1-c_{23})^2} \left(\dfrac{c_{23}+1}{2} + \dfrac{c_{23}}{1-c_{23}} \ln c_{23} \right)$

$$a_{3,3} = \dfrac{L_2}{3A_3 E} \phi_{33} + \dfrac{L_3}{3A_3 E} \qquad\qquad \text{(Eq.E6)}$$

where $\quad \phi_{33} = \dfrac{-3c_{23}}{(1-c_{23})^2} \left(\dfrac{c_{23}^2 - 4_{23} + 3}{2} + \ln c_{23} \right)$

$$a_{3,4} = a_{4,3} = \dfrac{L_3}{6A_3 E} \qquad\qquad \text{(Eq.E7)}$$

$$a_{4,4} = \dfrac{L_3}{3A_3 E} + \dfrac{L_4}{3A_4 E} \qquad\qquad \text{(Eq.E8)}$$

$$a_{4,5} = a_{5,4} = \dfrac{L_4}{6A_4 E} \qquad\qquad \text{(Eq.E9)}$$

$$a_{5,5} = \dfrac{L_4}{3A_4 E} + \dfrac{L_5}{3A_6 E} \phi_{55} \qquad\qquad \text{(Eq.E10)}$$

where $\quad \phi_{55} = \dfrac{3c_{56}}{(1-c_{56})^3} \left(\dfrac{3c_{56}^2 - 4c_{56} + 1}{2} - c_{56}^2 \ln c_{56} \right)$

and $\quad c_{56} = \dfrac{A_6}{A_5}$

$$a_{5,6} = a_{6,5} = \dfrac{L_5}{6A_6 E} \phi_{56} \qquad\qquad \text{(Eq.11)}$$

where $\quad \phi_{56} = \dfrac{6c_{56}}{(1-c_{56})^2} \left(\dfrac{c_{56}+1}{2} + \dfrac{c_{56}}{1-c_{56}} \ln c_{56} \right)$

$$a_{6,6} = \frac{L_5}{3A_6 E} \phi_{66} + \frac{L_6}{3A_7 E} \phi_{66}^1 \qquad \text{(Eq.E12)}$$

$$\text{where} \quad \phi_{66} = \frac{-3c_{56}}{(1-c_{56})^3} \left(\frac{c_{56}^2 - 4c_{56} + 3}{2} + \ln c_{56} \right)$$

$$\phi_{66}^1 = \frac{3c_{67}}{(1-c_{67})^3} \left(\frac{3c_{67}^2 - 4c_{67} + 1}{2} - c_{67}^2 \ln c_{67} \right)$$

$$\text{and} \quad c_{67} = \frac{A_7}{A_6}$$

$$a_{6,7} = a_{7,6} = \frac{L_6}{6A_7 E} \phi_{67} \qquad \text{(Eq.E13)}$$

$$\text{where} \quad \phi_{67} = \frac{6c_{67}}{(1-c_{67})^2} \left(\frac{c_{67}+1}{2} + \frac{c_{67}}{1-c_{67}} \ln c_{67} \right)$$

$$a_{7,7} = \frac{L_6}{3A_7 E} \phi_{77} + \frac{L_7}{3A_8 E} \phi_{77}^1 \qquad \text{(Eq.E14)}$$

$$\text{where} \quad \phi_{77} = \frac{-3c_{67}}{(1-c_{67})^3} \left(\frac{c_{67}^2 - 4c_{67} + 3}{2} + \ln c_{67} \right)$$

$$\phi_{77}^1 = \frac{3c_{78}}{(1-c_{78})^3} \left(\frac{3c_{78}^2 - 4c_{78} + 1}{2} - c_{78}^2 \ln c_{78} \right)$$

$$\text{and} \quad c_{78} = \frac{A_8}{A_7}$$

$$a_{7,8} = a_{8,7} = \frac{L_7}{6A_8 E} \phi_{78} \qquad \text{(Eq.E15)}$$

$$\text{where} \quad \phi_{78} = \frac{6c_{78}}{(1-c_{78})^2} \left(\frac{c_{78}+1}{2} + \frac{c_{78}}{1-c_{78}} \ln c_{78} \right)$$

$$a_{8,8} = \frac{L_7}{3A_8 E} \phi_{88} \qquad \text{(Eq.E16)}$$

$$\text{where} \quad \phi_{88} = \frac{-3c_{78}}{(1-c_{78})^3} \left(\frac{c_{78}^2 - 4c_{78} + 3}{2} + \ln c_{78} \right)$$

The flexibility coefficients corresponding to the axial loads in the stiffeners are computed noting that in each bay there are fourteen stiffener elements of the same length and cross-section area. For example, in bay 2,

$$a_{9,9} = a_{16,16} = a_{23,23} = a_{30,30} = a_{37,37} = a_{44,44} = a_{51,51} = a_{58,58}$$

$$= a_{65,65} = a_{72,72} = a_{79,79} = a_{86,86} = a_{93,93} = a_{100,100}$$

$$= \frac{L_1 + L_2}{3AE} = \frac{45}{3(4.5072)(10.5 \times 10^6)} = 316.9523 \times 10^{-9}$$

$$a_{10,10} = a_{17,17} = a_{24,24} = a_{31,31} = a_{38,38} = a_{45,45} = a_{52,52}$$

$$= a_{59,59} = a_{66,66} = a_{73,73} = a_{80,80} = a_{87,87} = a_{94,94}$$

$$= a_{101,101} = \frac{L_2 + L_3}{3AE} = \frac{70}{3(4.5072)(10.5 \times 10^6)} = 493.0383 \times 10^{-9}$$

$$a_{9,10} = a_{10,9} = a_{16,17} = a_{17,16} = a_{23,24} = a_{24,23} = a_{30,31} = a_{31,30}$$

$$= a_{37,38} = a_{38,37} = a_{44,45} = a_{45,44} = a_{51,52} = a_{52,51} = a_{58,59}$$

$$= a_{59,58} = a_{65,66} = a_{66,65} = a_{72,73} = a_{73,72} = a_{79,80} = a_{80,79}$$

$$= a_{86,87} = a_{87,86} = a_{93,94} = a_{94,93} = a_{100,101} = a_{101,100}$$

$$= \frac{L_2}{6AE} = \frac{35}{6(4.5072)(10.5 \times 10^6)} = 123.2596 \times 10^{-9}$$

Similar relations exist for the stiffener flexibility coefficients in the other bays. In order to utilize a digital computer to generate these flexibility coefficients, they may be expressed as follows:

$$a_{1+m+7n,\, 1+m+7n} = \frac{L_m + L_{m+1}}{3AE} \qquad\qquad \text{(Eq.E17)}$$

$$\text{where} \quad \begin{cases} m = 1,2,3,\ldots\ldots,7 \\ n = 1,2,3,\ldots\ldots,14 \end{cases}$$

and $\qquad a_{1+m+7n,2+m+7n} = a_{2+m+7n,1+m+7n} = \dfrac{L_{m+1}}{6AE}$ (Eq.E18)

where $\begin{cases} m = 1,2,3,\ldots\ldots,6 \\ n = 1,2,3,\ldots\ldots,14 \end{cases}$

In a similar manner, the flexibility coefficients corresponding to the shear flows may be expressed as

$$a_{106+m,106+m} = \dfrac{9.82L_m}{Gt}$$ (Eq.E19)

where $m = 1,2,3,\ldots\ldots,7$

and $\qquad a_{106+m+7n,106+m+7n} = \dfrac{10.46L_m}{Gt}$ (Eq.E20)

where $\begin{cases} m = 1,2,3,\ldots\ldots,7 \\ n = 1,2,3,\ldots\ldots,13 \end{cases}$

In equations E17, E18, E19 and E20, the constants have the following values:

$L_1 = 10$, $L_2 = L_3 = 35$, $L_4 = 19.5$, $L_5 = 28.8$, $L_6 = 29.6$, $L_7 = 12.1$,

$L_8 = 0$ and $A = 4.5072$, $E = 10.5 \times 10^6$, $G = 4 \times 10^6$, $t = 0.320$.

Equations E2 through E20 define all the non-zero elements in the a_{ij} matrix. There are 386 non-zero elements and 41,230 zero elements in the a_{ij} matrix.

The generalized force system shown in figure E2 contains 98 redundants. For this analysis, the normal forces in the stiffeners, q_9 through q_{106}, were selected as the 98 redundants. The unit external load matrix, denoted by $\left[g_{im}\right]$, is formed by applying unit loads in place of the external loads to the determinate structure obtained by removing the redundants. The number of rows in the g_{im} matrix is equal to the number of generalized forces. The number of columns in the g_{im} matrix is equal to the number of external loads. For the gen-

equal to the number of external loads. For the generalized force system used in this analysis, the g_{im} matrix is the 204 x 1 matrix given by equation E21.

$$
\left[g_{im} \right] = \left[g_{jn} \right] =
\begin{bmatrix}
g_{1,1} \\
g_{2,1} \\
g_{3,1} \\
\cdot \\
\cdot \\
\cdot \\
\cdot \\
g_{203,1} \\
g_{204,1}
\end{bmatrix}
\qquad \text{(Eq.E21)}
$$

where $\quad g_1 = g_2 = g_3 = g_4 = g_5 = g_6 = g_7 = g_8 = +1$

and $\quad g_9 = g_{10} = g_{11} = \cdots\cdots\cdots = g_{204} = 0$

The unit redundant force matrix, denoted by $\left[g_{ir} \right]$, is formed by applying unit forces in place of the redundants to the determinate structure. The number of rows in the g_{ir} matrix is equal to the number of generalized forces and the number of columns is equal to the number of redundants. In this analysis, the g_{ir} matrix is the 204 x 98 matrix given by equation E22.

$$
\left[g_{ir} \right] = \left[g_{js} \right] =
\begin{bmatrix}
g_{1,1} & g_{1,2} & g_{1,3} & \cdots\cdots & g_{1,98} \\
g_{2,1} & g_{2,2} & g_{2,3} & \cdots\cdots & g_{2,98} \\
\cdot & \cdot & \cdot & & \\
\cdot & \cdot & \cdot & & \\
\cdot & \cdot & \cdot & & \\
\cdot & \cdot & \cdot & & \\
\cdot & \cdot & \cdot & & \\
\cdot & \cdot & \cdot & & \\
\cdot & \cdot & \cdot & & \\
\cdot & \cdot & \cdot & & \\
g_{204,1} & g_{204,2} & g_{204,3} & \cdots\cdots & g_{204,98}
\end{bmatrix}
\qquad \text{(Eq.E22)}
$$

The values of the elements in the first column of the g_{ir} matrix are the values of the generalized forces when the first redundant, q_9, is set equal to unity. The values of the elements in the second column are obtained by setting the second redundant, q_{10}, equal to unity, etc. For example, when $q_9 = 1$, the non-zero elements in the first column are:

$$g_{2,1} = -1.000$$

$$g_{9,1} = +1.000$$

$$g_{107,1} = + \frac{1}{L_1} = +0.1000$$

$$g_{108,1} = - \frac{1}{L_2} = -0.028571$$

The remaining 200 elements in the first column are each equal to zero. The sign convention was chosen so that a positive normal force in the hold-down post or stiffeners represents a compressive force and a positive shear flow corresponds to a shear flow acting up on the left-hand edge of a panel element. As a further example, the elements in the eighth column of the g_{ir} matrix are obtained by setting the eighth redundant, q_{16}, equal to unity. The non-zero elements in the eighth column are:

$$g_{2,8} = -1.000$$

$$g_{16,8} = +1.000$$

$$g_{107,8} = g_{114,8} = + \frac{1}{L_1} = +0.1000$$

$$g_{108,8} = g_{115,8} = - \frac{1}{L_2} = -0.028571$$

The remaining 198 elements in the eighth column are each equal to zero.

In order to utilize a digital computer to generate the elements in the g_{ir} matrix, the elements of the g_{ir} matrix may be expressed as follows:

$$g_{9+n,1+n} = +1.0000 \tag{Eq.E23}$$

where $n = 0,1,2,3,\ldots\ldots,97$

$$g_{2+n,1+n+7m} = -1.0000 \tag{Eq.E24}$$

where $n = 0,1,2,\ldots,6$
and $m = 0,1,2,\ldots,13$

$$g_{107+7n,1+7m} = +\frac{1}{L_1} = +0.1000 \tag{Eq.E25}$$

$$g_{108+7n,1+7m} = -\frac{1}{L_2} = -0.028571 \tag{Eq.E26}$$

$$g_{108+7n,2+7m} = +\frac{1}{L_2} = +0.028571 \tag{Eq.E27}$$

$$g_{109+7n,2+7m} = -\frac{1}{L_3} = -0.028571 \tag{Eq.E28}$$

$$g_{109+7n,3+7m} = +\frac{1}{L_3} = +0.028571 \tag{Eq.E29}$$

$$g_{110+7n,3+7m} = -\frac{1}{L_4} = -0.051282 \tag{Eq.E30}$$

$$g_{110+7n,4+7m} = +\frac{1}{L_4} = +0.051282 \tag{Eq.E31}$$

$$g_{111+7n,4+7m} = -\frac{1}{L_5} = -0.034722 \tag{Eq.E32}$$

$$g_{111+7n,5+7m} = +\frac{1}{L_5} = +0.034722 \tag{Eq.E33}$$

$$g_{112+7n,5+7m} = -\frac{1}{L_6} = -0.033783 \tag{Eq.E34}$$

$$g_{112+7n,6+7m} = +\frac{1}{L_6} = +0.033783 \tag{Eq.E35}$$

$$g_{113+7n,6+7m} = -\frac{1}{L_7} = -0.082644 \tag{Eq.E36}$$

$$g_{113+7n,7+7m} = +\frac{1}{L_7} = +0.082644 \tag{Eq.E37}$$

In equations E25 through E37,

$m = 0,1,2,3,\ldots\ldots,13$
$n = 0,1,2,3,\ldots\ldots,m$

Equations E23 through E37 define the 1561 non-zero elements of the g_{ir}

matrix. The remaining 18431 elements are each equal to zero.

After forming the a_{ij}, g_{im} and g_{ir} matrices, a computer program is

required to perform the following matrix operations:

(1) Evaluate $\left[a_{rn}\right] = \left[g_{ri}\right]\left[a_{ij}\right]\left[g_{jn}\right]$ (Eq.E38)

where $\left[g_{ri}\right]$ is the transpose of $\left[g_{ir}\right]$ given by

equation E22,

$\left[a_{ij}\right]$ is given by equation E1,

and $\left[g_{jn}\right]$ is given by equation E21.

The a_{rn} matrix is a 98 x 1 matrix.

(2) Evaluate $\left[a_{rs}\right] = \left[g_{ri}\right]\left[a_{ij}\right]\left[g_{js}\right]$ (Eq.E39)

The a_{rs} matrix is a 98 x 98 symmetrical matrix.

(3) Evaluate the inverse of $\left[a_{rs}\right]$ denoted by $\left[a_{rs}^{-1}\right]$.

(4) Evaluate $\left[G_{rm}\right] = - \left[a_{rs}^{-1}\right]\left[a_{rn}\right]$ (Eq.E40)

The G_{rm} matrix is a 98 x 1 matrix.

(5) Evaluate $\left[G_{im}\right] = \left[g_{im}\right] + \left[g_{ir}\right]\left[G_{rm}\right]$ (Eq.E41)

The G_{im} matrix is a 204 x 1 matrix.

The elements of the G_{im} matrix represent the desired solution. The

204 elements of the G_{im} matrix are the values of the generalized forces

q_1, q_2, ... , q_{204} due to the application of a unit external load

q_1 = 1. The matrix operations may be checked by determining the matrix

product

$$\left[A_{rn}\right] = \left[g_{ri}\right]\left[a_{ij}\right]\left[G_{jn}\right]$$ (Eq.E42)

where $\left[G_{jn}\right] = \left[G_{im}\right]$. If the G_{im} matrix is correct, each element of the

A_{rn} matrix given by equation E42 will be equal to zero.

The computer programs required to generate the elements of the a_{ij}

and g_{ir} matrices were written by Mr. V. N. Eubanks of the Computer

Division of the GCMSFC. Mr. Eubanks also wrote the programs required to perform the necessary matrix operations.

The stress distribution in the panel was obtained from the computer solution for the G_{im} matrix. Since the G_{im} matrix gives the values of the generalized forces due to a unit external load, these values must be multiplied by the rebound load of 1.275×10^6 pounds to obtain the desired force distribution. From the computer results, the compressive stresses in the hold-down post at the indicated stations are:

$$f_0 = 12,189 \text{ psi}$$
$$f_{10^-} = 11,187 \text{ psi}$$
$$f_{10^+} = 22,037 \text{ psi}$$
$$f_{45} = 24,925 \text{ psi}$$
$$f_{80^-} = 20,683 \text{ psi}$$
$$f_{80^+} = 21,885 \text{ psi}$$
$$f_{99.5} = 19,922 \text{ psi}$$
$$f_{128.3} = 25,029 \text{ psi}$$
$$f_{157.9} = 37,653 \text{ psi}$$
$$f_{170} = 48,061 \text{ psi}$$

These stresses are compared with the hold-down post stresses obtained by Method II in figure E6.

The results for the compressive stresses in the stiffeners and the shear flows in the skin are given in Tables E1 and E2 respectively.

Table E1

Compressive Stresses in Stiffeners by Method I

Stif-fener	1	2	3	4	5	6	7	8	9	10	11	12	13	14
7	31,146	24,289	19,913	16,627	14,004	11,876	10,104	8,669	7,512	6,598	5,899	5,393	5,064	4,902
6	29,662	23,873	19,716	16,505	13,914	11,789	10,043	8,617	7,467	6,558	5,863	5,359	5,032	4,872
5	23,412	22,270	17,980	15,312	12,989	11,025	9,392	8,054	6,975	6,122	5,471	5,000	4,694	4,544
Bay 4	19,797	17,966	15,629	13,330	11,288	9,555	8,118	6,947	6,006	5,266	4,702	4,295	4,031	3,901
3	19,112	16,493	13,903	11,636	9,743	8,190	6,930	5,914	5,104	4,470	3,989	3,642	3,417	3,306
2	18,126	12,889	9,660	7,571	6,116	5,042	4,220	3,579	3,078	2,689	2,396	2,186	2,050	1,983
1	7,447	3,802	2,483	1,834	1,441	1,172	973	822	705	616	548	500	468	453

Notes: See figure E2 for numbering of bays and stiffeners.

Stresses are given in psi

Table E2

Shear Flows in Skin by Method I

Panel	1	2	3	4	5	6	7	8	9	10	11	12	13	14
7	1,011	458	303	230	184	151	124	101	81	64	49	36	23	11
6	2,656	1,704	1,245	981	799	658	542	443	357	282	216	156	101	50
5	3,285	2,720	2,267	1,899	1,589	1,323	1,093	894	721	569	435	315	204	101
Bay 4	3,464	3,305	2,965	2,566	2,174	1,817	1,502	1,227	988	780	596	431	280	138
3	4,412	4,285	3,821	3,275	2,751	2,284	1,879	1,530	1,229	968	739	534	346	170
2	7,511	6,135	4,965	4,041	3,302	2,700	2,202	1,784	1,428	1,123	856	618	401	197
1	10,485	7,129	5,415	4,296	3,470	2,820	2,292	1,854	1,483	1,165	888	641	415	204

Notes: Shear flows are given in pounds per inch.

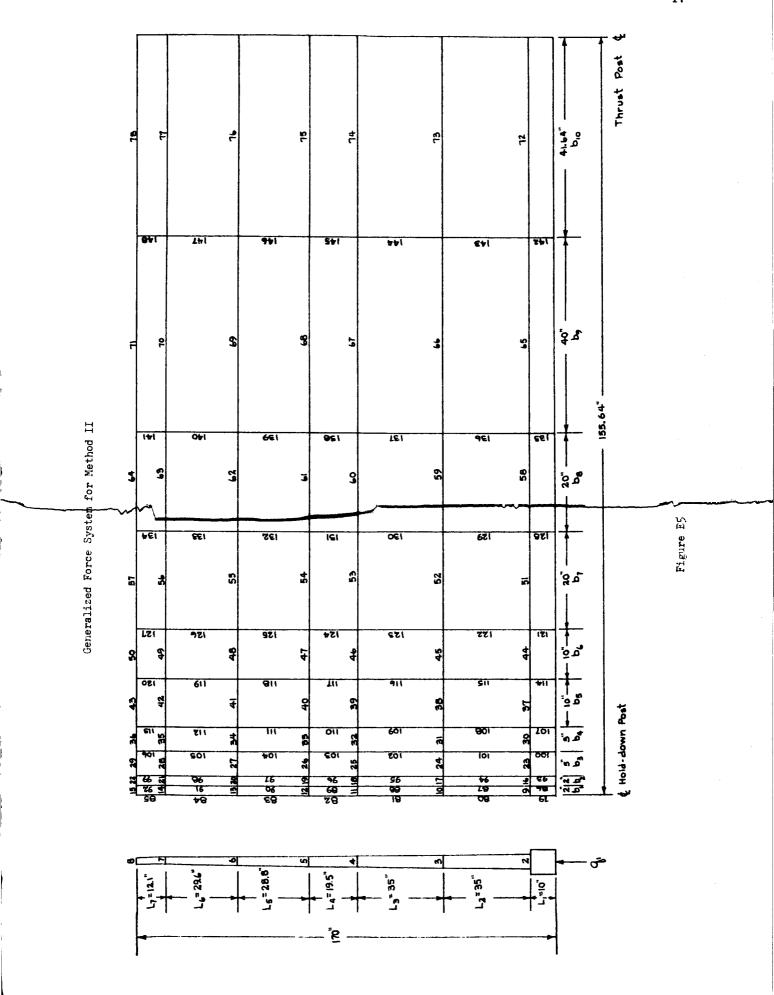Skin thickness = 0.320 inch.

See figure E2 for numbering of bays and stiffeners. Panel 1 is the panel between the hold-down post and stiffener 1, panel 2 is the panel between stiffeners 1 and 2, etc.

Method II

The analysis used in the second numerical example is referred to as Method II. The idealized structure used in this analysis consists of a hold-down post to which the load is applied and an unstiffened equivalent sheet. The analysis assumes that the hold-down post transmits only normal stresses while the equivalent sheet transmits both normal stresses and shearing stresses. The generalized force system used in this analysis is shown in figure E5. In figure E5, q_1 through q_8 represent the normal force in the hold-down post at the indicated stations, q_9 through q_{78} represent the normal force in the equivalent sheet at the indicated stations and q_{79} through q_{148} represent the shear flows in the equivalent sheet.

Since the stiffeners are uniformly spaced, the equivalent unstiffened sheet was obtained by distributing the total stiffener area over the width of the panel. In this manner, the equivalent unstiffened sheet was found to have a thickness of 0.42163 inch. This procedure appears to be justified by the assumption that the stiffened sheet does not buckle.

The normal force in the hold-down post was assumed to vary linearly between stations. The stress distribution in the equivalent sheet was assumed to vary in the manner discussed in Appendix D. For a given panel element, such as shown in figure D1, the normal force was assumed to vary linearly in the y-direction but remain constant in the x-direction while the shear flow was assumed to be constant in the y-direction but vary linearly in the x-direction.

Generalized Force System for Method II

Figure E5

This analysis assumes that the total strain energy consists of the sum of the following: (1) the strain energy due to the normal forces in the hold-down post, (2) the strain energy due to the normal forces in the equivalent sheet, (3) the strain energy due to the shear flow in the equivalent sheet. In this analysis, the strain energies due to the following forces are neglected: (1) normal forces in the skin that act normal to the stiffeners, (2) forces in the thrust post, (3) shearing forces in the posts, (4) forces in the intermediate rings. This analysis also assumes that the upper ring assembly serves as a rigid support.

For this analysis, the a_{ij} matrix is the 148 x 148 symmetrical matrix given by equation E43.

$$[a_{ij}] = \begin{bmatrix} a_{1,1} & a_{1,2} & a_{1,3} \cdots\cdots\cdots a_{1,148} \\ a_{2,1} & a_{2,2} & a_{2,3} \cdots\cdots\cdots a_{2,148} \\ \cdot & & \\ \cdot & & \\ \cdot & & \\ \cdot & & \\ \cdot & & \\ a_{148,1} & a_{148,2} & a_{148,3} \cdots\cdots\cdots a_{148,148} \end{bmatrix} \qquad (Eq.E43)$$

The elements of the a_{ij} matrix corresponding to the flexibility coefficients for the hold-down post are the same as those for Method I as given by equations E2 through E16. The flexibility coefficients corresponding to the normal forces in the equivalent sheet are:

$$\left. \begin{aligned} a_{2+7n,2+7n} &= \frac{L_1+L_2}{3b_n tE} \\[2mm] a_{3+7n,3+7n} &= \frac{L_2+L_3}{3b_n tE} \\[2mm] a_{4+7n,4+7n} &= \frac{L_3+L_4}{3b_n tE} \end{aligned} \right\} \quad (Eqs.E44)$$

$$a_{5+7n,5+7n} = \frac{L_4 + L_5}{3b_n tE}$$

$$a_{6+7n,6+7n} = \frac{L_5 + L_6}{3b_n tE}$$

$$a_{7+7n,7+7n} = \frac{L_6 + L_7}{3b_n tE}$$

$$a_{8+7n,8+7n} = \frac{L_7}{3b_n tE}$$

$$a_{2+7n,3+7n} = a_{3+7n,2+7n} = \frac{L_2}{6b_n tE}$$

$$a_{3+7n,4+7n} = a_{4+7n,3+7n} = \frac{L_3}{6b_n tE}$$

$$a_{4+7n,5+7n} = a_{5+7n,4+7n} = \frac{L_4}{6b_n tE}$$

$$a_{5+7n,6+7n} = a_{6+7n,5+7n} = \frac{L_5}{6b_n tE}$$

$$a_{6+7n,7+7n} = a_{7+7n,6+7n} = \frac{L_6}{6b_n tE}$$

$$a_{7+7n,8+7n} = a_{8+7n,7+7n} = \frac{L_7}{6b_n tE}$$

(Eqs. E44 cont'd)

In equations E44,

$$n = 1,2,3,\ldots\ldots\ldots,10$$

$$L_1 = 10,\ L_2 = L_3 = 35,\ L_4 = 19.5,\ L_5 = 28.8,\ L_6 = 29.6,\ L_7 = 12.1$$

$$b_1 = b_2 = 2,\ b_3 = b_4 = 5,\ b_5 = b_6 = 10,\ b_7 = b_8 = 20,\ b_9 = 40,$$

$$b_{10} = 41.64$$

$$E = 10.5 \times 10^6 \text{ and } t = 0.42163.$$

The flexibility coefficients corresponding to the shear flows in the equivalent sheet are:

$$a_{71+7n+m,\,78+7n+m} = a_{78+7n+m,\,71+7n+m} = \frac{L_m b_n}{6Gt}$$

$$a_{78+m,\,78+m} = \frac{2L_m}{3Gt}$$ (Eqs.E45)

$$a_{85+m+7(n-1),\,85+m+7(n-1)} = \frac{L_m(b_n+b_{n+1})}{3Gt}$$

In equations E45,

$m = 1,2,3,\ldots\ldots,7$

$n = 1,2,3,\ldots\ldots,9$

$L_1 = 10,\; L_2 = L_3 = 35,\; L_4 = 19.5,\; L_5 = 28.8,\; L_6 = 29.6,\; L_7 = 12.1$

$b_1 = b_2 = 2,\; b_3 = b_4 = 5,\; b_5 = b_6 = 10,\; b_7 = b_8 = 20,\; b_9 = 40$

$b_{10} = 41.64$

$G = 4 \times 10^6$ and $t = 0.42163$

Equations E2 through E16 along with equations E44 and E45 define the 408 non-zero elements of the a_{ij} matrix for Method II.

The generalized force system used in Method II contains 70 redundants.

The unit external load matrix, g_{im}, was formed by considering the normal forces in the sheet, g_9 through g_{78} as the 70 redundants. In this manner,

$$\left[g_{im}\right] = \left[g_{jn}\right] = \begin{bmatrix} g_1 \\ g_2 \\ g_3 \\ . \\ . \\ . \\ . \\ . \\ g_{148} \end{bmatrix}$$ (Eq.E46)

where $g_1 = g_2 = g_3 = g_4 = g_5 = g_6 = g_7 = g_8 = 1.0000$

$g_9 = g_{10} = g_{11} = \cdot \cdot \cdot \cdot \cdot \cdot = g_{148} = 0$

The unit redundant force matrix, g_{ir}, was formed by setting the redundants q_9 through q_{78} equal to unity. The values in column 1 of the g_{ir} matrix are the values of generalized forces when q_9 is equal to unity; the values in column 2 when q_{10} is equal to unity, etc. Defining the g_{ir} matrix as

$$\left[g_{ir} \right] = \left[g_{is} \right] = \begin{bmatrix} g_{1,1} & g_{1,2} & g_{1,3} & \cdot \cdot \cdot \cdot & g_{1,70} \\ g_{2,1} & g_{2,2} & g_{2,3} & & \\ \cdot & & & & \\ \cdot & & & & \\ \cdot & & & & \\ \cdot & & & & \\ g_{148,1} & \cdot \cdot \cdot \cdot \cdot \cdot \cdot \cdot \cdot \cdot \cdot & , & g_{148,70} \end{bmatrix} \qquad \text{(Eq.E47)}$$

The elements of the g_{ir} matrix are given by:

$$g_{8+n,n} = +1.0000 \qquad \text{(Eq.E48)}$$

where $n = 1,2,3,\ldots\ldots,70$

$$g_{1+n,n+7m} = -1.0000 \qquad \text{(Eq.E49)}$$

where $n = 1,2,3,\ldots\ldots,7$
and $m = 0,1,2,\ldots\ldots,9$

$$g_{79+7n,1+7m} = + \frac{1}{L_1}$$

$$g_{80+7n,1+7m} = g_{81+7n,2+7m} = - \frac{1}{L_2} = - \frac{1}{L_3}$$

$$\qquad \text{(Eqs.E50)}$$

$$g_{80+7n,2+7m} = g_{81+7n,3+7m} = + \frac{1}{L_2} = + \frac{1}{L_3}$$

$$g_{82+7n,3+7m} = - \frac{1}{L_4}$$

$$g_{82+7n,4+7m} = + \frac{1}{L_4}$$

$$g_{83+7n,4+7m} = - \frac{1}{L_5}$$

$$g_{83+7n,5+7m} = + \frac{1}{L_5}$$

$$g_{84+7n,5+7m} = - \frac{1}{L_6}$$ (Eqs.E50 cont'd)

$$g_{84+7n,6+7m} = + \frac{1}{L_6}$$

$$g_{85+7n,6+7m} = - \frac{1}{L_7}$$

$$g_{85+7n,7+7m} = + \frac{1}{L_7}$$

In equations E50,

$m = 0,1,2,........,9$

$n = 0,1,2,.......,m$

$L_1 = 10$, $L_2 = L_3 = 35$, $L_4 = 19.5$, $L_5 = 28.8$, $L_6 = 29.6$, $L_7 = 12.1$

Equations E48, E49, and E50 define the 855 non-zero elements of the g_{ir} matrix of equation E47.

The required matrix operations are the same as those for Method I given by equations E38, E39, E40, and E41. Equation E42 again serves as a check equation.

From the computer solution, the compressive stress in the hold-down post are:

$$f_0 \quad = 12,189 \text{ psi}$$
$$f_{10} \quad = 10,821 \text{ psi}$$
$$f_{10^+} = 21,317 \text{ psi}$$

$$f_{45} = 23{,}221 \text{ psi}$$

$$f_{80} = 19{,}178 \text{ psi}$$

$$f_{80^+} = 20{,}292 \text{ psi}$$

$$f_{99.5} = 18{,}408 \text{ psi}$$

$$f_{128.3} = 22{,}677 \text{ psi}$$

$$f_{157.9} = 32{,}554 \text{ psi}$$

$$f_{170} = 40{,}551 \text{ psi}$$

The compressive stresses in the hold-down post obtained by Method II are compared with those obtained by Method I in figure E6. The compressive stress distribution in the equivalent sheet and the shear flow distribution in the equivalent sheet, as determined by Method II, are given in Tables E3 and E4 respectively.

Table E3

Compressive Stresses in Equivalent Sheet by Method II

Bay	b_1	b_2	b_3	b_4	b_5	b_6	b_7	b_8	b_9	b_{10}
7	38,179	34,628	30,623	26,883	23,230	19,687	15,891	12,172	8,587	6,164
6	31,332	30,468	28,613	26,028	22,817	19,480	15,779	12,102	8,536	6,126
5	21,983	21,905	21,679	21,088	19,753	17,691	14,694	11,359	7,989	5,716
4	18,589	18,638	18,532	18,144	17,178	15,529	12,914	9,914	6,904	4,911
3	19,348	19,036	18,502	17,653	16,187	14,141	11,391	8,549	5,885	4,163
2	22,871	21,824	19,816	17,045	13,659	10,451	7,570	5,317	3,566	2,499
1	17,996	14,437	10,283	6,764	4,298	2,784	1,852	1,241	820	571

NOTES: See figure E5 for numbering of bays and panels. Stresses are given in psi.

Table E4

Shear Flows in Equivalent Sheet by Method II

Bay	y = 0	2	4	9	14	24	34	54	74	114
7	1,736	1,259	969	619	470	326	253	175	126	55
6	3,123	2,857	2,613	2,110	1,767	1,330	1,076	767	555	243
5	3,405	3,305	3,210	2,979	2,764	2,387	2,070	1,549	1,126	491
4	3,324	3,357	3,374	3,371	3,318	3,103	2,803	2,145	1,555	673
3	4,206	4,291	4,358	4,437	4,400	4,096	3,652	2,731	1,952	835
2	8,191	8,073	7,895	7,321	6,702	5,574	4,650	3,272	2,291	967
1	14,308	12,790	11,573	9,405	7,979	6,167	4,993	3,432	2,385	1,003

NOTES: y is measured in inches from the centerline of the hold-down post.

Shear flows are given in pounds per inch.

Equivalent sheet thickness = 0.42163 inch.

Compressive Stress in Hold-down Post
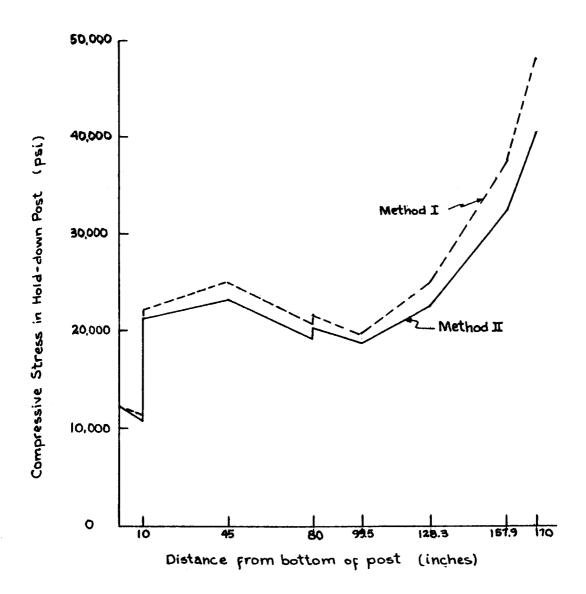
Figure E6

REFERENCES

A. Shear Lag

1. Akao, S.: Analysis of Shear Lag Problems by Means of Difference Equations. Technol. Rep. Osaka Univ., Vol. 9, March 1959, pp.91-99.

2. Anderson, R.A. and Houbolt, J.C.: Effect of Shear Lag on Bending Vibration of Box Beams. NACA TN 1583, 1948.

3. Argyris, J.H. and Cox, H.L.: Diffusion of Load into Flat Stiffened Panels of Varying Cross-Section. ARC (Great Britain), R. and M. No. 1969, 1944.

4. Argyris, J.H.: Diffusion of Symmetrical Loads into Stiffened Parallel Panels with Constant Area Edge Members. ARC (Great Britain), R. and M. No. 2038, 1944.

5. Argyris, J.H.: Diffusion of Anti-Symmetrical Concentrated End Loads and Edge Loads into Parallel Stiffened Panels and Analysis of Parallel Panels under Transverse Load. ARC (Great Britain), R. and M. No. 2882, 1946.

6. Argyris, J.H. and Dunne, P.C.: Diffusion in Flat Panels. Handbook of Aeronautics, No. 1, Structural Principles and Data, 4th edition. Pitman Publishing Company, New York, 1952, pp.271-281.

7. Benthem, J. P. and van der Vooren, J.: A Stress Diffusion Problem for a Wedge Shaped Plate with Three Stiffeners. Technical Report S.542, National Luchtvaartlaboratorium, Amsterdam, July 1959.

8. Borsari, P. and Yu, A.: Shear Lag in a Plywood Sheet-Stringer Combination Used for the Chord Member of a Box Beam. NACA TN 1443, 1948.

9. Chiarito, P.T.: Shear-Lag Tests of Two Box Beams with Flat Covers Loaded to Destruction. NACA Wartime Report L-307, 1942.

10. Chiarito, P.T.: Shear-Lag Tests of Two Box Beams with Corrugated Covers Loaded to Failure. NACA Wartime Report L-482, 1944.

11. Cox, H.L., Smith, H.E. and Conway, C.G.: Diffusion of Concentrated Loads into Monocoque Structures. ARC (Great Britain), R. and M. No. 1780, 1937.

12. Cox, H.L.: Diffusion of Concentrated Loads into Monocoque Structures. General Considerations with Particular Reference to Bending Load Distribution. ARC (Great Britain), R. and M. No. 1860, 1938.

13. Cox, H.L.: Stress Analysis of Thin Metal Construction. Journal of the Royal Aeronautical Society, Vol. 44, March 1940, pp. 231-282.

14. Davenport, W.W. and Kruszewski, E.T.: A Substitute-Stringer Approach for Including Shear-lag Effects in Box-Beam Vibrations. NACA TN 3158, 1954.

15. Duberg, J.E.: Comparison of an Approximate and an Exact Method of Shear Lag Analysis. NACA Wartime Report L-310, 1944.

16. Duncan, W.J.: Diffusion of Load in Certain Sheet-Stringer Combinations. ARC (Great Britain), R. and M. No. 1825, 1938.

17. Ebner, H.: The Strength of Shell Bodies-Theory and Practice. NACA TM 838, 1937.

18. Ebner, H. and Koller, H.: Calculation of Load Distribution in Stiffened Cylindrical Shells, NACA TM 866, 1938.

19. Fine, M.: A Comparison between Plain and Stringer Reinforced Sheet from the Shear Lag Standpoint. ARC (Great Britain), R. and M. No. 2648 1941.

20. Fine, M. and Hopkins, G.: Stress Diffusion Adjacent to Gaps in the Inter-spar Skin of a Stressed-Skin Wing. ARC (Great Britain), R. and M. no. 2618, 1942.

21. Goland, M.: Shear Lag Solutions for Sheet-Stringer Panels by Means of a Hydrodynamic Analogy. Journal of the Aerospace Sciences, Vol. 27. April 1960, pp. 291-295, 303.

22. Goodey, W.J.: Stress Diffusion Problems. Aircraft Engineering, Vol. 18, 1946, pp.195-198, 227-230. 234, 271-276, 313-316, 343-346, 385-389.

23. Heck, O.S. and Ebner, H.: Formulae and Methods of Calculation of the Strength of Plate and Shell Structures in Aeroplane Construction. Journal of the Royal Aeronautical Society, Vol. 40, 1936, p. 769.

24. Hildebrand, F.B. and Reissner, E.: Least Work Analysis of the Problem of Shear Lag in Box Beams. NACA TN 893, 1943.

25. Hildebrand, F.B.: The Exact Solution of Shear Lag Problems in Flat Panels and Box Beams Assumed Rigid in the Transverse Direction. NACA TN 894, 1943.

26. Hoff, N.J.: Stresses in a Reinformced Monocoque Cylinder Under Concentrated Summetric Transverse Loads. Journal of Applied Mechanics, Vol. 11, No. 4, December 1944, p. A235.

27. Hoff, N.J.: Concentrated Load Effects in Reinforced Monocoque Structures. Reissner Anniversary Volume. J.W. Edwards, Ann Arbor, Michigan, 1949, pp. 277-289.

28. Kempner, J.: Recurrence Formulas and Differential Equations for Stress Analysis of Cambered Box Beams. NACA TN 1466, 1947.

29. Kuhn, P.: Stress Analysis of Beams with Shear Deformation of the Flanges. NACA TR 608, 1937.

30. Kuhn, P.: Bending Stresses in Box Beams as Influenced by Shear Deformation. Journal of the Society of Automotive Engineers, Vol. 43, August 1938, pp. 319-324.

31. Kuhn, P.: Approximate Stress Analysis of Multi-stringer Beams with Shear Deformation of the Flanges. NACA TR 636, 1938.

32. Kuhn, P.: A Recurrence Formula for Shear-Lag Problems. NACA TN 739, 1939.

33. Kuhn, P. and Brilmyer, H.G.: An Approximate Method of Shear Lag Analysis for Beams Loaded at Right Angles to the Plane of Symmetry of the Cross Section. NACA Wartime Report L-324, 1943.

34. Kuhn, P. and Chiarito, P.: Shear Lag in Box Beams-Methods of Analysis and Experimental Investigations. NACA TR 739, 1943.

35. Kuhn, P. and Peterson, J.P.: Shear Lag in Axially Loaded Panels. NACA TN 1728, 1948.

36. Kuhn, P.: Shear Lag. Stresses in Aircraft and Shell Structures. McGraw-Hill Book Company, Inc., 1956, pp. 101-154, 354-382.

37. Levy, R.S.: Effect of Bending Rigidity of Stringers Upon Stress Distribution in Reinforced Monocoque Cylinder Under Concentrated Transverse Loads. Journal of Applied Mechanics, Vol. 15, No. 1 March 1948, pp. A30-A36.

38. Lovett, B.B.C. and Rodee, W.F.: Transfer of Stress from Main Beams to Intermediate Stiffeners in Metal Sheet Covered Box Beams. Journal of the Aeronautical Sciences, Vol. 3, October 1936, pp. 426-430.

39. Ness, N.: Application of Southwell's Method to the Shear Lag Analysis of a Monocoque Cylinder. Thesis, Polytechnic Institute of Brooklyn, October 1943.

40. Newell, J.S. and Reissner, E.: Shear Lag in Corrugated Sheets Used for the Chord Member of A Box Beam. NACA TN 791, 1941.

41. Newton, R.E.: Electrical Analogy for Shear Lag Problems. Proceedings of the Society for Experimental Stress Analysis, Vol. 2, No. 2 1945, pp. 71-80.

42. Peterson, J.P.: Shear-lag Tests on a Box Beam with a Highly Cambered Cover in Tension. NACA Wartime Report L-106, 1945.

43. Reissner, E.: On the Problem of Stress Distribution in Wide-Flanged Box Beams. Journal of the Aeronautical Sciences, Vol. 5, June 1938, pp. 295-299.

44. Reissner, E.: The Influence of Taper on the Efficiency of Wide-Flanged Box Beams. Journal of the Aeronautical Sciences, Vol. 7, June 1940, pp. 353-357.

45. Reissner, E.: Least Work Solutions of Shear Lag Problems. Journal of the Aeronautical Sciences. Vol. 8, May 1941, pp. 284-291.

46. Reissner, E.: Analysis of Shear Lag in Box Beams by the Principle of Minimum Potential Energy. Quarterly of Applied Mechanics, Vol. 4, October 1946, pp. 268-278.

47. Ross, R.D.: An Electrical Computer for the Solution of Shear-lag and Bolted-joint Problems. NACA TN 1281, 1947.

48. Salerno. V.L.: The Applicability of Saint-Venant's Principle to Reinforced Monocoque Structures. Reissner Anniversary Volume. J. W. Edwards, Ann Arbor, 1949, pp. 290-299.

49. Sibert, H.: Effect of Shear Lag upon Wing Strength. Journal of the Aeronautical Sciences. Vol. 6, August 1939, pp. 418-420.

50. Smith, H.E.: Diffusion of Load in Sheet-stringer Structures having a Tapered Central Stringer. ARC (Great Britain), R. and M. no. 1862, 1938.

51. White, R.J. and Antz, H.M.: Tests on the Stress Distribution in Reinforced Panels. Journal of the Aeronautical Sciences, Vol. 3, April 1936, pp. 209-212.

52. Williams, D. and Fine, M.: Stress Distribution in Reinforced Flat Sheet, Cylindrical Shells and Cambered Box Beams under Bending Actions. ARC (Great Britain), R. and M. No. 2099, 1940.

53. Williams, D., Starkey, R.D. and Taylor, R.H.: Distribution of Stress between Spar Flanges and Stringers for a Wing under Distributed Loading. ARC (Great Britain), R. and M. No. 2098, 1939.

54. Winny. H.F.: The Distribution of Stress in Monocoque Wings. ARC (Great Britain), R. and M. No. 1756, 1938.

B. Matrix Applications

55. Argyris, J.H.: Energy Theorems and Structural Analysis. Aircraft Engineering, Vol. 26, 1954, pp. 347-356, 383-387, 394, Vol. 27, 1955, pp. 42-58, 80-94, 125-134, 145-158.

56. Argyris, J.H. and Kelsey, S.: The Matrix Force Method of Structural Analysis and Some New Applications. ARC (Great Britain), R. and M. No. 3034, 1956.

57. Argyris, J.H. and Kelsey, S.: The Analysis of Fuselages of Arbitrary Cross-section and Taper. Aircraft Engineering, Vol. 31 1959, pp. 62-74, 101-112, 133-143, 169-179, 192-203, 244-256, 272-283.

58. Benscoter, S.U.: The Partioning of Matrices in Structural Analysis. Journal of Applied Mechanics, Vol. 15, No. 4, December 1948 pp. 303-307.

59. Benscoter, S.U. and Gossard, M.L.: Matrix Methods for Calculating Cantilever Beam Deflections. NACA TN 1827, 1949.

60. Boley, B.A.: Numerical Methods in the Calculation of Elastic Instability. Journal of the Aeronautical Sciences, Vol. 14, January 1947, pp. 337-348.

61. Bruhn, E.F. and Schmitt, A.F.: Analysis and Design of Aircraft Structures, Volume One, Analysis for Stress and Strain. Tri-State Offset Company, Cincinnati, 1958, pp. A7.22-A7.23.

62. Crichlow, W. J. and Haggenmacher, G.W.: The Analysis of Redundant Structures by the Use of High-Speed Digital Computers. Journal of the Aerospace Sciences, Vol. 27, August 1960, pp. 595-606, 614.

63. Chirico, M., Klein, B. and Owens, A.: Automatic Digital Matric Structural Analysis. Proceedings of the Western Joint Computer Conference, 1959, pp. 272-276.

64. Denke, P.H. and Boldt, I.V.: General Digital Computer Program for Static Stress Analysis. Proceedings of the Western Computer Conference, 1955.

65. Denke, P.H.: A Matric Method of Structural Analysis. Proceedings of the Second U.S. National Congress of Applied Mechanics, 1954, pp. 445-451.

66. Denke, P.H: The Matric Solution of Certain Nonlinear Problems in Structural Analysis. Journal of the Aeronautical Sciences, Vol. 23, March 1956, pp. 231-236.

67. Duberg, J.E.: A Numerical Procedure for the Analysis of Stiffened Shells. Journal of the Aeronautical Sciences, Vol. 16, August 1949. pp. 451-462.

68. Dunholter, R.J.: Some Fundamental Theorems of Structural Mechanics in Vector Notation. Journal of Engineering Education, Vol. 37, No. 3, November 1946, pp. 207-209.

69. Falkenheimer, H.: Systematic Analysis of Redundant Elastic Structures by Means of Matrix Calculus. Journal of the Aeronautical Sciences, Vol. 20, April 1953, pp. 293-294.

70. Hoff, N.J., Libby, P.A. and Klein, B.: Numerical Procedures for the Calculation of the Stresses in Monocoques. II. Calculation of the Bending Moments in Fuselage Frames. NACA TN 998, 1946.

71. Hoff, N.J., Klein, B. and Libby, P.A.: Influence Coefficients of Curved Bars for Distortions in Their Own Plane. NACA TN 999, 1946.

72. Jensen, V.P. and Dill, D.G.: Matrix Methods of Analysis Applied to Wing Structures. Douglas Aircraft Co. Report E.S. 6480, January 1944.

73. Kempner, J.: Application of a Numerical Procedure to the Stress Analysis of Stringer-Reinforced Panels. NACA Wartime Report L-11, 1945.

74. Klein, B.: A Simple Method of Matric Structural Analysis. Journal of the Aeronautical Sciences, Vol. 24, January 1957, pp. 39-46.

75. Klein, B.: A Simple Method of Matric Structural Analysis. Part II-Effects of Taper and a Consideration of Curvature. Journal of the Aeronautical Sciences, Vol. 24, November 1957, pp. 813-820.

76. Klein, B.: Application of the Witte Rearranging Method to a Typical Structural Matrix. Journal of the Aeronautical Sciences, Vol. 25, May 1958, pp. 342-343.

77. Klein, B.: A Simple Method of Matric Structural Analysis: Part III Flexible Frame and Stiffened Cylindrical Shell Analysis. Journal of the Aeronautical Sciences, Vol. 25, June 1958, pp. 385-394.

78. Klein, B.: A Simple Method of Matric Structural Analysis: Part IV Nonlinear Problems. Journal of the Aerospace Sciences, Vol. 26, June 1959, pp. 351-359.

79. Klein, B.: Simultaneous Calculation of Influence Coefficients and Influence Loads for Arbitrary Structures. Journal of the Aerospace Sciences, Vol. 26, July 1959, pp. 451-452.

80. Klein, B.: A Simple Method of Matric Structural Analysis: Part V - Structures Containing Plate Elements of Arbitrary Shape and Thickness. Journal of the Aerospace Sciences, Vol. 27, November 1960, pp. 859-866.

81. Klein, B.: Application of a New Matrix Method to Vibration Analysis of Structures. Journal of the Aerospace Sciences, Vol. 29, March 1962, pp. 350-351.

82. Klein, B.: A Simple Method of Matric Structural Analysis: Part VI - Bending of Plates of Arbitrary Shape and Thickness Under Arbitrary Normal Loading. Journal of the Aerospace Sciences, Vol. 29, March 1962.pp. 306-310, 322.

83. Kron, G.: Solving Highly Complex Elastic Structures in Easy Stages. Journal of Applied Mechanics, Vol. 22, No. 2, June 1955, pp. 235-244.

84. Langefors, B.: Matrix Methods for Redundant Structures. Journal of the Aerospace Sciences, Vol. 20, April 1953, pp. 292-293.

85. Langefors, B.: Analysis of Elastic Structures by Matrix Transformation with Special Regard to Semi-monocoque Structures. Journal of the Aeronautical Sciences, Vol. 19, July 1952, pp. 451-458.

86. Levy, S.: Computation of Influence Coefficients for Aircraft Structures with Discontinuities and Sweepback. Journal of the Aeronautical Sciences, Vol. 14, October 1947, pp. 547-560.

87. Magnus, D.E. and Eisen, D.: Digital Programs for the Structural Analyses of Homogeneous Conical and Ogival Shells under Mechanical and Thermal Loading. General Applied Science Labs, Scientific Report No. 17, January 1960.

88. McMinn, S.J.: Matrices for Structural Analysis, John Wiley and Sons, Inc., New York, 1962.

89. Melosh, R.: Matrix Methods of Structural Analysis. Journal of the Aerospace Sciences, Vol. 29, March 1962, pp. 365-366.

90. Morris, J.: On the Nature of Least Work Equations in Structures. Journal of the Royal Aeronautical Society, Vol. 51, March 1947, pp. 327-333.

91. Pei-ping, C.: Matrix Analysis of Pin-Connected Structures. Proceedings of the American Society of Civil Engineers, Vol. 73, 1947 pp. 1475-1482.

92. Przemieniecki, J.S.: Matrix Analysis of Shell Structures with Flexible Frames. Aeronautical Quarterly, Vol. 9, 1958, pp. 361-394.

93. Salerno, V.L.: A Revised Recurrence Formula For A Ring-Stiffened Circular Cylinder Under Concentrated Loads. Grumman Aircraft Engineering Corporation Research Report RE-94, 1958.

94. Salerno, V.L.: Closed Form Solution For A Ring-Stiffened Circular Cylinder Under Concentrated Loads. Grumman Aircraft Engineering Corporation Research Report RE-96, 1958.

95. Samson, Jr., C.H.: Further Comments on the Inversion of Large Structural Matrices. Journal of the Aerospace Sciences, Vol. 29, March 1962, pp. 373-374.

96. Schmid, L.J.: Flexibility Matrices for Elements of Constant and Variable Cross-Sections under General Loading. Australian Aeronautical Research Labs, Structures and Materials Report 279, 1961.

97. Turner, M.J., Clough, R.W., Martin, H.C. and Topp, L. J.: Stiffness and Deflection Analysis of Complex Structures. Journal of the Aeronautical Sciences, Vol. 23, September 1956, pp. 805-823, 854.

98. Wehle, Jr., L. B. and Lansing, W.: A Method for Reducing the Analysis of Complex Redundant Structures to a Routine Procedure. Journal of the Aeronautical Sciences, Vol. 19, October 1952, pp. 677-684.